Wageningen University & Research
Department of Genetics

Mechanisms and Impacts of Succinate Dehydrogenase Inhibitor Resistance in *Aspergillus fumigatus*: Exploring Fitness Costs and Compensatory Mutations.

Date: 20.09.2024

Student: Tolga Bayraktar

Program: Master Biotechnology/Cellular and Molecular Biotechnology

MSc Thesis Genetics: GEN82000

Supervisor: Spyros Kanellopoulos (Laboratory of Genetics, Wageningen University & Research)

Examiners: Ben Auxier (Laboratory of Genetics, Wageningen University & Research), René Boesten (Laboratory of Genetics, Wageningen University & Research)

Chair Group: Plant Sciences Group (PSG), Laboratory of Genetics

Table of Contents

Abstract

Succinate dehydrogenase inhibitors (SDHIs) are widely used alongside agricultural fungicides to inhibit the growth of fungal plant pathogens. However, the application of these fungicides in agricultural environments can indirectly effect *Aspergillus fumigatus*, leading to the development of resistance over time. This study investigates the mechanisms of SDHI resistance in *A. fumigatus* and explores the fitness costs associated with resistance, as well as potential compensatory mutations in environmental resistant variants. Genomic analysis of environmental samples collected from Dutch compost heaps identified specific single nucleotide polymorphisms (SNPs) in the *sdh*B and *sdh*C genes (*sdh*B^{H270Y} and *sdh*C^{S105I}), conferring resistance to boscalid and fluopyram, respectively. Using CRISPR-Cas9 technology, these mutations were introduced into the SDHI-sensitive strain AfiR974 to assess fitness effects, including radial growth under normoxic and hypoxic conditions, as well as fungal biomass production in liquid culture. No statistically significant fitness costs were observed for the *sdh*C^{S105I} mutation. However, sexual crossing experiments and fungal burden assays suggested fitness costs in strains carrying the *sdh*B^{H270Y} mutation, along with potential compensatory mutations that mitigate these effects. This project highlights the complexity of SDHI resistance mechanisms by identifying resistant variants within a population of 84 environmental isolates and linking genotype to phenotype through the identification of mutations that select for resistance to boscalid and fluopyram. Computational analysis predicted the 3D structure of the SdhC protein, illustrating how the *sdh*C^{S105I} mutation impacts fluopyram binding. Building on these findings, future research should explore the role of the *sdh*B^{H270Y} mutation, as well as the compensatory mutations that may mitigate associated fitness costs and further advance *A. fumigatus* resistance research.

Keywords

Aspergillus fumigatus, Succinate dehydrogenase inhibitors (SDHIs), Fungicide resistance, Single nucleotide polymorphisms (SNPs), Fitness costs, Compensatory mutations

1. Introduction

1.1 Challenges of fungal pathogens in agriculture and the role of antifungals in enhancing crop productivity.

The agricultural industry is continually confronted with significant hurdles in optimizing crop yields and enhancing harvest quality (Ricroch et al., 2016). Biotic stressors account for a substantial proportion of crop losses and pose a critical threat to global food production capacities (Berger et al., 2017). Fungal pathogens are some of the most prominent biotic stressors (Price et al., 2015). These are known to secrete mycotoxins, which pose significant health risks, including DNA damage, growth, and immune system impairment, and genetic alterations (Awuchi et al., 2022). In response to the challenges posed by fungal pathogens, the agricultural industry has turned to fungicides, which directly eliminate or suppress fungal growth (Dzhavakhiya et al., 2012). This use of fungicides has proven to be effective in controlling plant diseases caused by fungal pathogens during crop development (Sallach et al., 2021). As a result of fungicide use, farms benefit from increased productivity, longer storage life of crops, and improved overall quality of harvested plants (Jampilek, 2016).

1.2 Unintended effects of agricultural azole use: the emergence of resistance in *A. fumigatus* and its impacts on human health.

Among the various fungicides used in agriculture, azoles are particularly prominent due to their broad-spectrum activity and cost-efficiency (Hof, 2001). The application of agricultural azoles in controlling the spread of fungal plant pathogens may inadvertently expose other fungal species within the same environment, such as *A. fumigatus*, to these chemicals (Sen et al., 2022). *A. fumigatus*, a saprophytic fungus belonging to the *Aspergillus* genus and the Fumigati section, plays a crucial role in the global cycling of carbon and nitrogen (Sugui et al., 2015). Due to its ubiquity and the production of hydrophobic airborne conidia that can withstand harsh environmental conditions, the inhalation of these conidia poses a lethal risk to immunocompromised individuals (Nywening et al., 2020). Infections can result in various responses, including allergic syndromes, aspergilloma, and invasive aspergillosis (Camps et al., 2012). In clinical practice, clinical azoles are the treatment of choice for invasive aspergillosis (Brauer et al., 2019). However, prolonged azole therapy for IA has been associated with the emergence of azole-resistant *A. fumigatus* strains among patient isolates (Howard et al., 2006). In addition to developing resistance through prolonged treatment, *A. fumigatus* can also acquire resistance due to the continuous selection pressure exerted by azoles utilized in agriculture (Snelders et al., 2009). This occurs as *A. fumigatus* coexists with the plant pathogens targeted by azoles, leading to an evolutionary adaptation (Jørgensen & Heick, 2021).

1.3 Combined use of fungicides: mechanisms of cross-resistance and multi-fungicide resistance in *A. fumigatus*.

Besides the use of agricultural azoles, a variety of other fungicides are commonly used in combination in the field, including methyl benzimidazole carbamates (MBCs), demethylation inhibitors (DMIs), quinone outside inhibitors (QoIs), and succinate dehydrogenase inhibitors (SDHIs) (Gonzalez-Jimenez et al., 2021). While only the use of azoles can lead to the selection of cross-resistance in *A. fumigatus*, the concurrent use of these additional fungicides can lead to developing multi-fungicide resistance (Kang et al., 2022). Cross-resistance occurs in response to fungicides with similar chemical structures, conferring resistance to specific groups of fungicides (Leroux et al., 2010). In contrast, multi-fungicide resistance is non-specific, enabling resistance to a broad range of fungicides, regardless of variations in molecular structure (Hu & Chen, 2021). The primary mechanisms underlying resistance to various fungicide include: (i) structural alterations in target proteins, (ii) overexpression of target proteins, which allows intracellular concentrations to exceed the inhibitory levels of the fungicide, (iii) increased activity of efflux transporters that reduce intracellular fungicide concentrations, thereby diminishing their toxic effects (Berger et al., 2017), and (iv) activation of alternative pathways that compensate for the inhibition of targeted pathways, ensuring the continuation of essential cellular processes (Leroux et al., 2010). These mechanisms are not exclusively linked to a single type of fungicide. For example, structural alterations and target protein overexpression may occur in response to fungicides with similar molecular structures, while efflux transporter overexpression can confer resistance to diverse fungicides, regardless of their structural differences (Engle & Kumar, 2024).

1.4 SDHI resistance in *A. fumigatus*: target-site alterations, fitness costs, and the need for comprehensive research.

Among the fungicides used in combination to enhance effectiveness, SDHIs specifically target the critical cellular process of succinate dehydrogenase (SDH) in the Krebs cycle (Sang & Lee, 2020). SDH, also known as complex II, is an enzyme complex comprising four subunits (SdhA, SdhB, SdhC, and SdhD) that regulate cellular respiration by catalyzing the oxidation of succinate to fumarate (Figure 1) (Pearce et al., 2019). The SDH complex is divided into two main domains: the membrane-peripheral domain and the membrane-anchor domain (Shao et al., 2020). The peripheral domain contains the hydrophilic subunits SdhA and SdhB, while the membrane-anchor domain includes the hydrophobic subunits SdhC and SdhD (Avenot & Michailides, 2010).

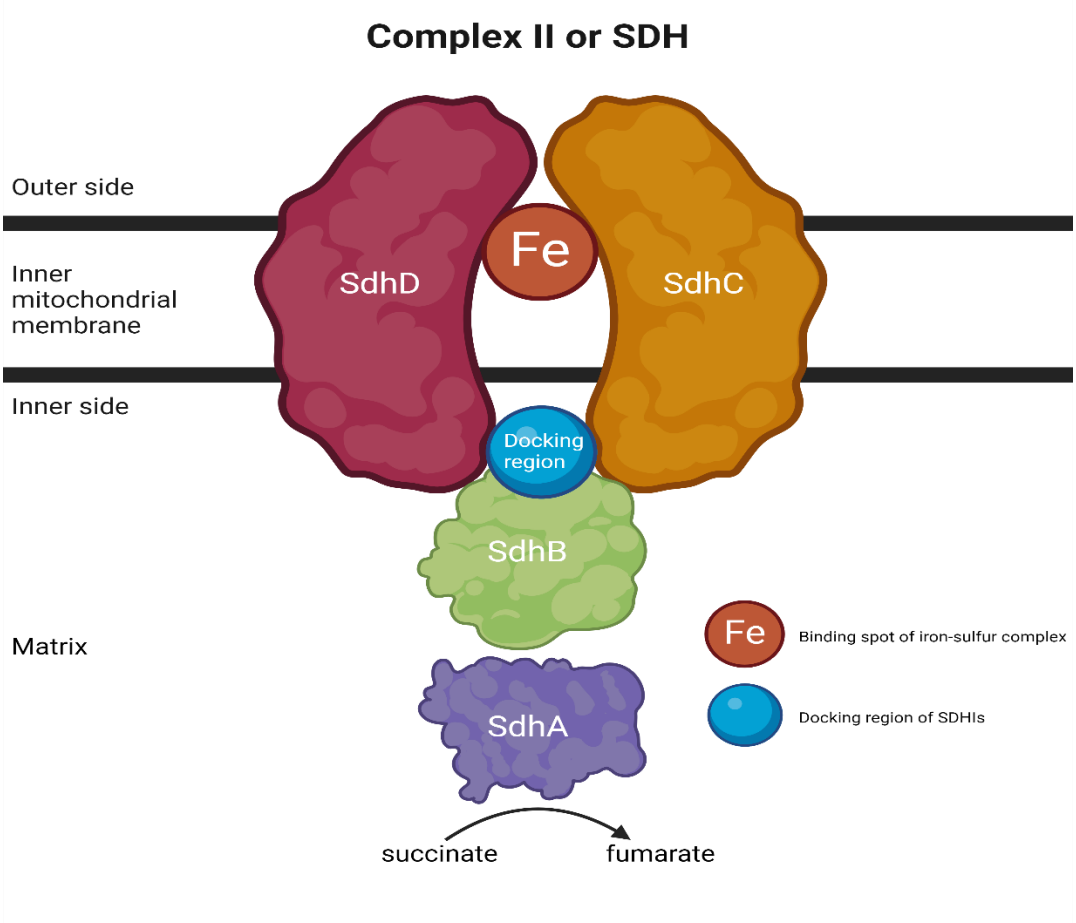

Figure 1 - Schematic structure of SDH protein complex (Complex II) as well as the protein subunits with iron-sulfur complex binding site and SDHI binding site. (Adapted from Leroux et al., 2010).

SDHIs function by binding to and disrupting the activity of three subunits of the SDH protein: SdhB, SdhC, and SdhD, blocking the activation of the iron-sulfur complex, thereby inhibiting subunit function (Leroux et al., 2010). As a result, SNPs often arise as target-site alterations within the genes that encode their corresponding subunits, either preventing the binding of SDHIs or reducing the affinity of the fungicide for the protein (Sang & Lee, 2020). For instance, SNPs within the genes encoding the SDH subunits (*sdh*B, *sdh*C, and *sdh*D) can lead to amino acid substitutions, which may hinder the binding of these fungicides to the protein subunits (Miyamoto et al., 2010), thereby diminishing their efficacy (Vielba-Fernández et al., 2021). However, these substitutions can alter the protein's conformation and impair its original function (Hawkins & Fraaije, 2018) . This may come with fitness costs, as this protein complex plays a critical role in regulating respiration and is highly conserved through evolution (Her & Maher, 2015). Consequently, SDHI-resistant strains may exhibit fitness penalties, such as reduced growth rate, increased sensitivity to oxidative stress, decreased hyphal growth, and lower conidial production compared to sensitive strains (Hawkins & Fraaije, 2018). Complementing this, fitness costs associated with SNPs that confer SDHI resistance have been observed in fungal plant pathogens

such as *Corynespora cassiicola* with *sdh*B^{H278Y} (Shi et al., 2021), and *Botrytis cinerea* with *sdh*B^{H272Y} (Lalève et al., 2014), resulting in reduced growth, decreased virulence, and increased sensitivity to oxidative stress.

1.5 Investigating fitness costs and compensatory mutations in SDHI-resistant *A. fumigatus*: expanding our understanding of fungal resistance evolution.

While fitness costs associated with SDHI resistance have been documented in fungal plant pathogens, their impact on *A. fumigatus* remains underexplored. This highlights the need for a deeper understanding of how SDHI resistance affects fungal fitness and adaptation mechanisms in *A. fumigatus*. Furthermore, the potential role of compensatory mutations in mitigating these fitness costs remains largely uncharted.

Our research seeks to address these critical gaps by emphasizing the fitness costs associated with SDHI resistance and investigating the possible emergence of compensatory mutations within *A. fumigatus*. To achieve these goals, we will test environmental *A.* fumigatus samples collected from farms in the Netherlands, identify resistance-conferring SNPs, and induce these mutations in a sensitive isolate via CRISPR-Cas9-mediated mutagenesis. Fitness assessments will include radial growth (under both normoxic and hypoxic conditions), production of fungal biomass, and the *Galleria mellonella* infection model to evaluate virulence. By doing so, we aim to enrich our understanding of the evolutionary dynamics of SDHI resistance, contributing valuable insights into the adaptability of this human pathogen in the face of fungicidal pressure. Building on this approach, we hypothesize that target-site alterations in the SDHB and SDHC protein subunits, which confer resistance to SDHIs in A. fumigatus, will result in measurable fitness costs, including reduced radial growth, virulence, and stress response. However, we further anticipate that compensatory mutations may emerge to mitigate these fitness disadvantages, allowing the fungus to regain its competitive edge.

2. Materials and Methods

2.1 *A. fumigatus* Isolate Preparation

The initial step involves the preparation of fungal stocks from environmental isolates. A total of 84 *A. fumigatus* environmental isolates (see Appendix 1) were retrieved from -80°C storage. Each isolate was transferred from its corresponding Eppendorf tube into slants containing Malt Extract Agar (MEA) supplemented with 0.1% (m/v) $CuSO_4$ (30 g of malt extract and 15 g of agar in 1L deionized water using sterile cotton swabs for transfer. The inoculated slants were incubated at 37°C for 2 days.

2.2 SDHI Sensitivity Assessment

To assess SDHI resistance, 84 *A. fumigatus* isolates were inoculated onto minimal media containing boscalid or fluopyram at 1 mg/L and 5 mg/L concentrations, with control media containing no fungicides. Fluopyram (Sigma-Aldrich, CAS No. 658066-35-4) and boscalid

(Sigma-Aldrich, CAS No. 188425-85-6) were each resuspended in 1 mL of PBS to prepare a stock solution of 10 mg/mL. For plates with a final concentration of 5 mg/L, 200 µL of the stock solution was added to 400 mL of minimal media. For plates with a final concentration of 1 mg/L, 40 µL of the stock solution was added to 400 mL of minimal media. The minimal medium agar (1 L) consisted of $NaNO_3$ (6.0 g, using a 1M stock solution), KH_2PO_4 (1.5 g), $MgSO_4 \cdot 7H_2O$ (0.5 g), KCl (0.5 g), 100 µL of 10,000x trace element stock solution ($FeSO_4$/$ZnSO_4$/$CuSO_4$/$MnCl_2 \cdot H_2O$), sucrose (8.55 g), and agar (15 g), adjusted to pH 5.8 with deionized water. To prepare 1 L of 1x PBS, 8 g of NaCl, 0.2 g of KCl, 1.44 g of Na_2HPO_4, and 0.24 g of KH_2PO_4 were dissolved in 800 mL of deionized water. The pH was adjusted to 7.4 using a pH meter and either HCl or NaOH as needed. The final volume was then adjusted to 1 L with deionized water. Spore concentrations were measured using a CASY Model TT Cell Counter and Analyzer (OMNI Life Science). For each isolate, a 10 µL aliquot of spore suspension was mixed with 10 mL of CASY Buffer, and spore concentrations were determined. The measurement was conducted with a capillary diameter of 45 µM, and the evaluation was performed using a cursor range from 1.68 µM to 5.00 µM. Based on the CML value, the spore suspensions were diluted to obtain 10 µL aliquots containing 1 x 10^6 spores, which were used for inoculation. Plates were incubated at 37°C. Fungal growth was monitored daily for 3 days. Resistance was determined by comparing growth on SDHI-containing media to media containing no fungicides. Resistance was determined by comparing the growth of environmental isolates to the control strain, AfiR974, which is sensitive to fungicides.

2.3 Bioinformatic Analysis

To investigate the genetic basis of SDHI resistance, sequences from the *sdh*A*, sdh*B*, sdh*C, and *sdh*D genes of 84 *A. fumigatus* environmental isolates were mapped on their respective counterparts (gene IDs: 3512570, 3511321, 3509950, and 3511446, respectively) from the reference strain *A. fumigatus* Af293 using Geneious software version 2024.0. *A. fumigatus* Af293 has been shown to not be resistant to any SDHI fungicides (Cite reference or experiment where we tested it). The analysis focused on identifying both synonymous and non-synonymous SNPs in exonic regions, which are directly involved in coding for protein structures (Table 1).

Table 1 **-** List of resistant profiles of environmental resistant variants to fluopyram and boscalid. R = resistant, S = sensitive.

Gene	SNP	Nucleotide	Reference Number	Sample ID	Fluopyram	Boscalid
*sdh*C	S105I	AGC -> ATC	35	48A6	R	S
*sdh*C	S105I	AGC -> ATC	36	48A5	R	S
*sdh*C	S105I	AGC -> ATC	37	36B7	R	S
*sdh*C	S105I	AGC -> ATC	38	76A18	R	S
*sdh*C	S105I	AGC -> ATC	45	35CS28	R	S
*sdh*C	S105I	AGC -> ATC	48	78C2	R	S

*sdh*B	H270Y	CAC -> TAC	39	11A6	S	R
*sdh*B	H270Y	CAC -> TAC	46	66A3	S	R

2.3.1 Protein-Ligand Docking Model

To simulate the binding patterns of fluopyram to the SdhC protein subunit, the 3D structure of the SdhC protein from AfiR974 and AfiR974 *sdh*C^{S105I} mutant (see Appendix 4) was predicted using the I-TASSER server (Zhang, 2008). The 3D structure of fluopyram was retrieved from PubChem (Compound ID: 11158353). Binding pattern analysis between fluopyram and the predicted SdhC structure was performed using the CB-Dock tool (Liu et al., 2020). Secondary structure confidence and solvent accessibility scores of SdhC protein of AfiR974 and AfiR974 *sdh*C^{S105I} mutant are obtained from I-TASSER server (Zhang, 2008).

2.4 Primer Design and Polymerase Chain Reaction Setup

To facilitate the detection of *sdh*B^{H270Y} and *sdh*C^{S105I} mutations in *A. fumigatus* isolates, specific primers were developed. Using sequences retrieved from the NCBI database for the Af293 reference strain, primers were designed with Primer-BLAST, targeting the regions containing these SNPs (Table 2). These primers were then used in a polymerase chain reaction (PCR) to amplify the corresponding DNA regions. PCR was performed using a Bio-Rad T100 Thermal Cycler. The PCR reaction mixture totaled 25 µL and consisted of 12.5 µL of PCRBIO VeriFi Mix, 1 µL of DNA template, 1 µL each of forward and reverse primers (10 µM), and 9.5 µL of distilled water. The cycling conditions were an initial denaturation at 95°C for 1 minute, followed by 34 cycles of denaturation at 95°C for 15 seconds, annealing at 68°C for 15 seconds, and extension at 72°C for 30 seconds, concluding with a final extension at 72°C for 3 minutes.

2.4.1 *A. fumigatus* DNA Preparation

To prepare DNA from *A. fumigatus* spores for PCR, we utilized a heat-shock method adapted from (Fraczek et al. (2019). A 30 µL of spore suspension was subjected to heat treatment at 95°C for 15 minutes, followed by rapid cooling at -80°C for 10 minutes.

2.4.2 Gel Electrophoresis

1% agarose gel was prepared by dissolving 3 g of agarose in 300 mL of 1X TAE buffer. The 1X TAE buffer was obtained by diluting 200 mL of 50X TAE buffer with 10 L of deionized water. After the agarose was fully dissolved, 15 µL of ethidium bromide (EtBr) was added to the gel for DNA visualization. A 1 kb DNA Ladder (Thermo Fisher, Catalog #SM0311) was used as a reference to compare the sizes of the DNA products. The gels were run at 100 V for 30 minutes using a gel electrophoresis system (Bio-Rad Sub-Cell GT System). Gels were imaged at a BioRad Gel Doc XR+ station and processed with Image Lab™ Software (Bio-Rad Laboratories).

Table 2 - Primers designed for amplification of *sdh*B and *sdh*C regions in *A. fumigatus* isolates.

Primer ID	Sequence (5' – 3')	Direction	Amplicon Size (base pair)	Annealing Temperature (Tm)	Target
TB001_sdhCFw	GGGGATAGTAGACCAAGAGAGT	Forward	982	66°C	*sdh*C
TB001_sdhCRv	CAGCGTCTTGCCTGAGTTTG	Reverse	982	66°C	*sdh*C
TB_002_sdhBFw_L	ATGGGTGTGACCTTGGCCTCCA	Forward	2913	72°C	*sdh*B
TB_002_sdhBRv_L	TGGTTGGGTTAGGGCCGAGGAG	Reverse	2913	72°C	*sdh*B
TB_003_sdhCFw	GGGGATAGTAGACCAAGAGAGT	Forward	982	66°C	*sdh*C
TB_003_sdhCRv	CAGCGTCTTGCCTGAGTTTG	Reverse	982	66°C	*sdh*C
TB_004_sdhB_H270Y_Fw	ACACCAAGACCGAGGATGTG	Forward	614	68°C	*sdh*B
TB_004_sdhB_H270Y_Rv	TCAATTGCCCCAGAAGAAAACG	Reverse	614	68°C	*sdh*B

2.5 Sexual Spore Crossing

Environmental *A. fumigatus* resistant variants (Table 1) were crossed with high fertility (see Appendix 2) sensitive strains (Figure 3) to investigate genetic linkage between SNPs and resistance phenotypes (O'Gorman et al., 2009). Oatmeal agar plates were prepared using BD DIFCO™ Dehydrated Culture Media: Oatmeal Agar (500 g), consisting of oatmeal (60 g/L) and agar (12.5 g/L). For 1 L of medium, 60 g of oatmeal and 12.5 g of agar were dissolved in 1 L of distilled water. Plates were labeled according to the cross-combination map (see Appendix 2). Spores from each strain were inoculated on opposite sides of the plates using fresh stocks (see Appendix 3). Plates were wrapped in parafilm, loosely covered with aluminum foil, and placed in plastic bags to maintain humidity during incubation at 30°C for three months. Cleistothecia were observed under a light microscope at 10x magnification, collected using a sterile inoculation loop, and cleaned on water agar. The water agar was prepared following the protocol from Hardy Diagnostics (n.d.). Agar 1.5% preparation. Retrieved July 2, 2024, from https://hardydiagnostics.com/media/assets/product/documents/Agar_1_5.pdf. After collection, cleistothecia were transferred to 1 mL Eppendorf tubes containing saline, crushed, and heat-shocked at 70°C for two hours to eliminate asexual spores. A 10 µL aliquot of the spore suspension was inoculated onto complete media (CM) plates supplemented with 1% Triton and incubated at

37°C for two days. Saline solution (1 L) was prepared by dissolving 9 g of NaCl in 1 L of deionized water. Complete medium agar (1 L) was composed of $NaNO_3$ (6.0 g), KH_2PO_4 (1.5 g), $MgSO_4 \cdot 7H_2O$ (0.5 g), KCl (0.5 g), neopeptone (2.0 g), vitamin assay casamino acids (1.0 g), yeast extract (1.0 g), ribonucleic acid (0.3 g), agar (15 g), and 100 µL of 10,000x trace element stock solution ($FeSO_4/ZnSO_4/CuSO_4/MnCl_2 \cdot 4H_2O$). The solution was adjusted to 1 L with deionized water, and the pH was set to 5.8. Before use, 12.5 mL of 2M sucrose (or 1% glucose) and 2.0 mL of vitamin solution were added.

Table 3 - Succsessful crosses between High Fetility and Environemntal Samples. High fertility sensitive isolates: 46A23, 67A2, AfiR974, AfiR964. Environmental boscalid resistant variants: 11A6 and 66A3. Environmental fluopyram resistant variants: 35CS28, 78C2, 76A18, and 48A5.

Number	Crossing Type
2	46A23 X 11A6
3	46A23 X 35CS28
5	46A23 X 78C2
9	67A2 X 66A3
11	AfiR974 X 48A5
12	AfiR974 X 11A6
15	AfiR974 X 78C2
31	AfiR964 X 76A18

2.6 Fungal Burden Assay in *G. mellonella*

To evaluate the virulence of the environmental resistant variants (Table 1) and high fertility sensitive strain, AfiR974, a fungal burden assay was conducted using *G. mellonella* larvae. Twenty larvae per treatment group were injected with 20 µL of spore suspension containing 5×10^6 spores/mL using single-use insulin syringes (Carl Roth). Following infection, the larvae were incubated at 37°C in complete darkness. Humidity levels were not controlled during the experiment. Larvae were monitored daily for survival and signs of melanization over seven days, with dead larvae identified by complete lack of motility and intense melanization. Larvae were reared at Wageningen University & Research, Laboratory of Genetics, by Jordi and Elia.

2.7 CRISPR-Cas9 Mediated Mutagenesis and Transformation in *A. fumigatus*

2.7.1 gRNA and Single-Stranded Donor DNA Design

Guide RNAs (gRNAs) were designed for the induction of *sdh*C^{S105I} in high fertility and fungicide-sensitive *A. fumigatus* strains (AfiR974 and AfiR964). Additional gRNAs were designed to target synonymous and non-synonymous mutations in the *sdh*B and *sdh*C genes (Table 4). Single-stranded donor DNA (ssdDNA) templates were prepared to facilitate homology-directed repair (HDR) and introduce the desired SNPs (Table 5). gRNAs, ssdDNAs, were designed based on the web-based gRNA designing software, EuPaGDT (http://grna.ctegd.uga.edu/) (Peng & Tarleton, 2015). The software used for gRNA design followed by the protocol outlined by (van

Rhijn et al. (2020) in Development of a marker-free mutagenesis system using CRISPR-Cas9 in Aspergillus fumigatus, with adaptations for this study. Unlike the original protocol, this study targeted the *sdh*C gene, centering the SNPs with 50 bp upstream and 50 bp downstream flanking the target region. gRNAs were selected based on total scores and GC content, and those closest to the target integration sites were manually chosen for the transformation experiment (Table 4).

2.7.2 AfiR974 Protoplast Preparation

Protoplasts were prepared from *A. fumigatus* high fertility and sensitive strain, AfiR974, using a modified protocol based on (Hearn et al. (1980). Spores of AfiR974 were incubated in 40 mL of complete media (CM) with $2x10^8$ spores at 30°C and 100 rpm for 16 hours. After incubation, the cultures were filtered through Miracloth using a sterile funnel, and the mycelium was washed twice with CM. The washed mycelium was then transferred to a flask containing 32 mL of CM-protoplasting solution. The CM-protoplasting solution was prepared by making a 5% VinoTaste FCE (Novo Nordisk) in a 50-50 mix of KCl-citric acid solution and complete media. For one strain, 1.6 g of VinoTaste was dissolved in 16 mL of CM and 16 mL of KCl-citric acid solution. The KCl-citric acid solution was prepared by dissolving 8.2 g of KCl and 2.1 g of citric acid monohydrate in 50 mL of deionized water. The pH was adjusted to 5.8 using 10M KOH, and the volume was made up to 100 mL with deionized water.

The flask was incubated at 30°C and 100 rpm for 3 hours. Hyphae digestion was checked after 1.5 hours under a microscope at 40x magnification, and protoplast formation was observed. The undigested hyphae were filtered through a 40 µm cell strainer and centrifuged at 1,800 × g for 10 minutes. The supernatant was discarded, and the protoplasts were resuspended in 2 mL of 0.6 M KCl. 0.6 M KCl was prepared by dissolving 4.47 g of KCl in 100 mL of deionized water. The protoplasts were centrifuged again at 2,400 × g for 3 minutes. The supernatant was removed, and the pellet was washed twice in 0.6 M KCl. Finally, the protoplasts were resuspended in 1 mL of 0.6 M KCl and 50 mM $CaCl_2$. The 0.6 M KCl - 50 mM $CaCl_2$ solution was prepared by dissolving 4.47 g of KCl and 0.74 g of $CaCl_2 \cdot 2H_2O$ in 100 mL of deionized water. The protoplasts were adjusted to a final concentration of 5×10^6 protoplasts/mL by dilution with PBS-Tween20 buffer. For 1 L of 1x PBS-Tween20, 8 g of NaCl, 0.2 g of KCl, 1.44 g of Na_2HPO_4, and 0.24 g of KH_2PO_4 were dissolved in 800 mL of water. 5 mL of a 10% [v/v] Tween20 stock solution was added, and the pH was adjusted to 7.4. The final volume was adjusted to 1 L with water.

2.7.3 CRISPR-Cas9 Transformation

The CRISPR-Cas9 transformation and gRNA preparation were performed according to an in-house protocol developed by Wageningen University & Research, Laboratory of Genetics, authored by Francisca Reyes Marquez. These procedures were carried out using the protoplasts prepared from *A. fumigatus* strains as described above. To prepare gRNAs, crRNA and tracrRNA were resuspended in Nuclease-Free Duplex Buffer to a final concentration of 100 µM. For each RNA, a duplex solution was prepared by mixing 4 µL of 100 µM Alt-R CRISPR-Cas9 crRNA with 4 µL of 100 µM Alt-R CRISPR-Cas9 tracrRNA, and 4 µL of nuclease-free water, for a final volume

of 12 µL. The solution was heated to 95°C for 5 minutes and gradually cooled to room temperature (25°C) using a thermal cycler with a ramp rate of 1°C per second. For transformation, protoplasts were adjusted to a final concentration of 5×10^6 protoplasts/mL in 0.6 M KCl and 50 mM $CaCl_2$. Each transformation reaction consisted of 1.5 µL of gRNA duplex solution, 5 µg of Cas9 protein, and 500 ng of repair template (ssDNA). The mixture was incubated on ice for 10 minutes before adding 100 µL of protoplast suspension to the reaction. A 25% (w/v) PEG 4000 solution (protoplast suspension) was prepared by dissolving 25 g of PEG 4000 in 100 mL of 0.6 M KCl. The solution was stirred gently until the PEG 4000 was fully dissolved. The transformation mixture was incubated on ice for an additional 20 minutes before being transferred to 500 µL of PEG 4000 solution. The mixture was incubated for 5 minutes at room temperature, followed by a further 5-minute incubation on ice. Transformed protoplasts were plated on YPS plates supplemented with hygromycin. The YPS agar plates (1 L) consisted of yeast extract (20 g), Tris base (0.6057 g), peptone (5 g), sucrose (342.3 g), and agar (15 g), with the pH adjusted to 6.0 using 1 M sucrose. The final volume was adjusted to 1 L with deionized water. Supplementation of hygromycin maintained at a final concentration of 500 µg/mL. A hygromycin stock solution was prepared at a concentration of 1000 mg/mL, and 175 µL of the stock was added to 400 mL of YPS medium.

Table 4 - List of gRNAs for synonymous and non-synonymous mutations.

gRNA ID	Sequence	Length	Target Gene	Amino Acid Substitution
SdhCS105IgRNA	TCTAGCGCTCACCGTATCACCGG	23	*sdh*C	S105I (AGC -> ATC)
SdhBCntrlgRNA	TGTCGTCAAGGACTTGGTCCCGG	24	*sdh*B	P168P (CCG -> CCC)
SdhCCntrlgRNA	GAGCCAATCCAGGTGATCTGGGG	24	*sdh*C	T100T (ACC -> ACT)
Tolga gRNA #1	TCTACCGTCCCCAGATCACCTGG	23	*sdh*C	S105I (AGC -> ATC)
Tolga gRNA #2	ATCACCGGCATTGCTCTTTCTGG	23	*sdh*C	S105I (AGC -> ATC)

Table 5 - List of designed ssdDNAs to induce either synonymous or non-synonymous mutations, with the specific SNP in bold.

ssdDNA ID	Sequence	Length	Gene
SdhCS105Issd	TTTCCCCTCACCTCTCCATCTACCGTCCCCAGATCACCTGGA TTGGCTCTA**t**CGCTCACCGTATCACCGGCATTG CTCTTTCTGGCTCCTTGTACCTTTTCGC	103	*sdh*C
SdhBCntrlssd	GTCGCGTATCTACCCGTTGCCTCACACCTATGTCGTCAAGG	102	*sdh*B

	ACTTGGTCCC**c**GATCTGACCTACTTCTACAAGC AATACAAGTCCATCAAGCCTTACCTGCA		
SdhCCntrlssd	AAAAGGTACAAGGAGCCAGAAAGAGCAATGCCGGTGATAC GGTGAGCGCTAGAGCCAATCCA**a**GTGATCTGGGGAC GGTAGATGGAGAGGTGAGGGGAAACGGGGCGATTCAAGCG	116	*sdh*C
Tolga ssDNA #1	TGAATCGCCCCGTTTCCCCTCACCTCTCCATCTACCGTCCCCAGA TCACCTGGATTGGCTCTA**t**CGCTCACCGTATCACCGG CATTGCTCTTTCTGGCTCCTT	103	*sdh*C
Tolga ssDNA #2	CCCGTTTCCCCTCACCTCTCCATCTACCGTCCCCAGATC ACCTGGATTGGCTCTA**t**CGCTCACCGTATCACC GGCATTGCTCTTTCTGGCTCCTTGTACCTTT	103	*sdh*C

2.7.4 Mutation Analysis via Restriction Digestion

To confirm the presence of the *sdh*C^{S105I} mutation in *A. fumigatus* AfiR974 transformant, restriction digestion followed by gel electrophoresis was performed. The PCR-amplified *sdh*C region was digested using AfeI restriction enzyme. The 20 µL digestion reaction consisted of 5 µL of PCR product, 2 µL of rCutSmart buffer, 0.1 µL of AfeI enzyme, and 12.9 µL of distilled water.

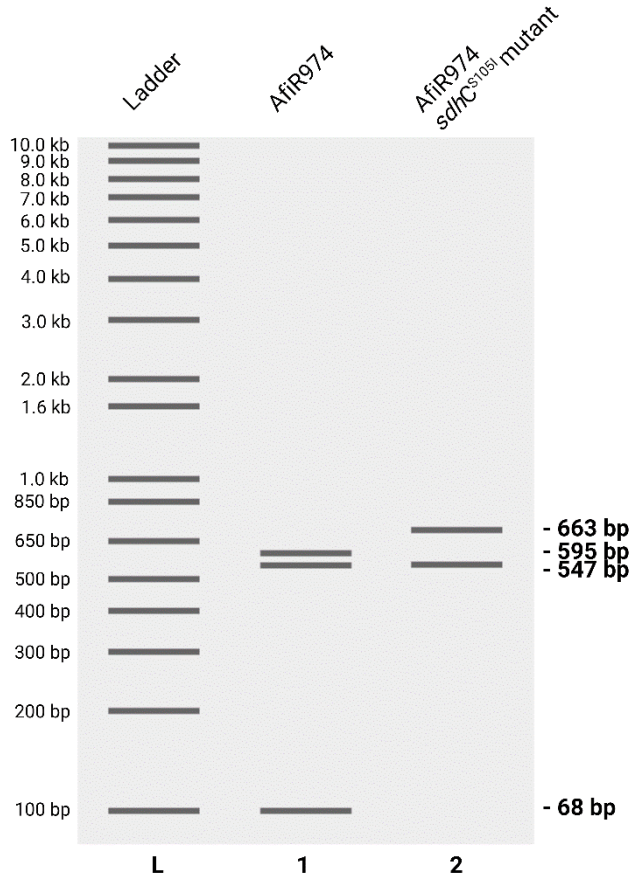

Figure 2 - Restriction digestion was performed using the AfeI enzyme to analyze the *sdh*C gene in *A. fumigatus* isolates. DNA from the AfiR974 strain and the AfiR974 *sdh*C^{S105I} mutant was digested with AfeI. In the AfiR974 strain, two AfeI restriction sites were present, producing three fragments (68 bp, 547 bp, and 595 bp). In the *sdh*C^{S105I} mutant, a nucleotide change within the *sdh*C gene caused the loss of one restriction site, producing two fragments (547 bp and 663 bp). Digested products were separated on an agarose gel, which was run at 100 V for 45 minutes.

The mixture was incubated at 37°C for 15 minutes, followed by enzyme deactivation at 65°C for 30 minutes. To visualize the digested DNA, the products were resolved on a 1% agarose gel by electrophoresis at 100 V for 45 minutes (Figure 2). A 1 kb DNA Ladder (Thermo Fisher, Catalog #SM0311) was used as a reference to compare the sizes of the digested DNA fragments.

Induced CRISPR-Cas9 mutants, AfiR974 *sdh*C^{S105I} and AfiR974 *sdh*B^{H270Y}, were tested for resistance to fluopyram and boscalid, respectively. Sterilin standard 90mm Petri dishes (Fisher Scientific, Cat. No. 11759252) were filled with minimal media containing 5 mg/L of fluopyram or 5 mg/L of boscalid, depending on the treatment. This setup was used to confirm the CRISPR-Cas9-mediated mutagenesis. Resistance was determined by comparing the growth of the CRISPR-Cas9 mutants to the control strain, AfiR974, which is sensitive to both fungicides.

2.8 Radial Growth Assay Under Normoxic and Hypoxic Conditions

Radial growth was assessed to evaluate the fitness effects of the *sdh*C^{S105I} mutation in *A. fumigatus* under both normoxic and hypoxic conditions. Fungal spores (1×10^5 spores/mL) were inoculated onto minimal media supplemented with glucose, with 10 µL of spore suspension applied to each plate. Plates were incubated at 37°C for 3 days, with radial growth measurements recorded every 24 hours. For hypoxic conditions, plates were placed in candle jars to create a low-oxygen environment. All experiments were performed in triplicate.

2.9 Dry Fungal Biomass Production

Dry fungal biomass production was measured to assess the fitness effects of the *sdh*C^{S105I} mutation. Six *A. fumigatus* isolates including high fertility and sensitive strains (AfiR964 and AfiR974), environmental fluopyram-resistant variants (35CS28, 48B6, and 36B7) and AfiR974 *sdh*C^{S105I} mutant, were inoculated into 50 mL of liquid minimal media at 1 x 10^5 spores/mL. Cultures were incubated at 37°C in a shaker set at 200 rpm for 3 days. The experiment was performed in triplicate, and biomass was collected via Büchner Funnel, dried at 60°C for 7 days, and weighed.

3. Results

3.1 SDHI Sensitivity Assay: Fluopyram and Boscalid Resistance and Frequency of Resistant Isolates

An SDHI sensitivity assay using fluopyram and boscalid was performed on 84 *A. fumigatus* isolates (see Appendix 1) to differentiate resistant isolates from sensitive ones. The assay identified isolates capable of growing under the selective pressure of these fungicides, indicating resistance (Figure 3A). No isolates demonstrated resistance to both fluopyram and boscalid simultaneously.

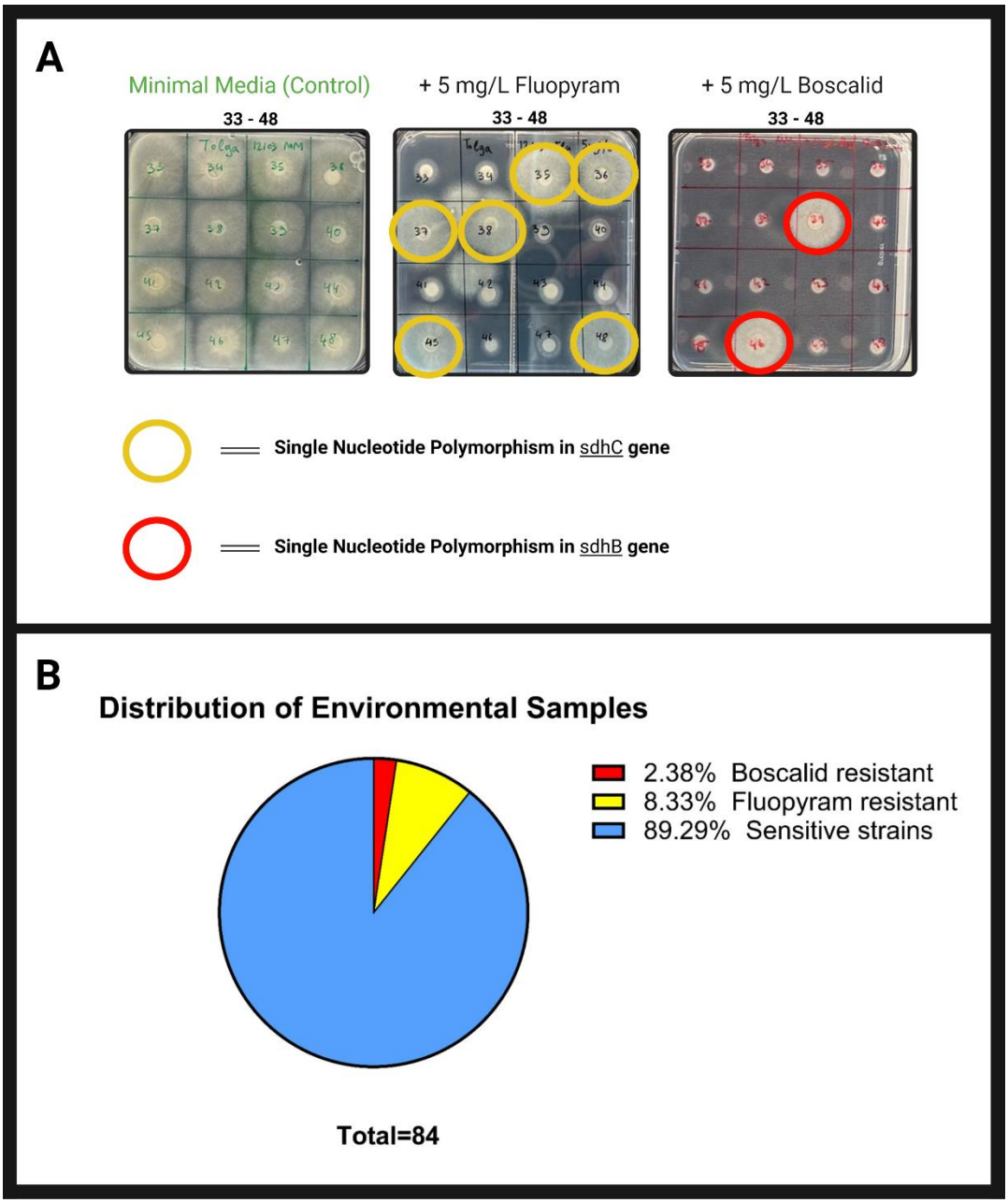

Figure 3 - Identified environmental resistant isolates. A, Selection of resistant environmental variants on 5 mg/L boscalid and 5 mg/L fluopyram. Resistant isolates are highlighted with circles: yellow for fluopyram resistance and red for boscalid resistance. **B,** Frequency of the identified environmental resistant isolates among the population of 84 environmental isolates (see Appendix 1). The red area represents the identified environmental boscalid resistant variants within the population, the yellow area represents the identified environmental fluopyram resistant variants, and the remaining blue area indicates the environmental strains that are sensitive to both fungicides.

Among the environmental samples, the frequency of isolates resistant to fluopyram was 8.33%, while for boscalid, it was 2.38% (Figure 3B).

3.2 Comparative Analysis of Environmental Resistant Variants for Detection of Resistance Conferring SNPs

One of the primary objectives of this study was to identify potential SNPs associated with resistance in *A. fumigatus* within the population of 84 environmental isolates (see Appendix 1).

Table 6 - List of SNPs selecting resistance in environmental *A. fumigatus* variants. This table shows the location of mutations (in either *sdh*C or *sdh*B gene), the corresponding nucleotide changes, associated sample IDs, and the resistance profiles for fluopyram.

Gene	SNP	Nucleotide	Sample ID	Reference Number	Fluopyram	Boscalid
*sdh*C	S105I	AGC -> ATC	48A6	35	R	S
*sdh*C	S105I	AGC -> ATC	48A5	36	R	S
*sdh*C	S105I	AGC -> ATC	36B7	37	R	S
*sdh*C	S105I	AGC -> ATC	76A18	38	R	S
*sdh*C	S105I	AGC -> ATC	35CS28	45	R	S
*sdh*C	S105I	AGC -> ATC	78C2	48	R	S
*sdh*B	H270Y	CAC -> TAC	11A6	39	S	R
*sdh*B	H270Y	CAC -> TAC	66A3	46	S	R

According to the resistant isolates identified in Figure 3A, comparative analysis had been performed to identify if there is any SNPs present. The bioinformatic analysis revealed that the environmental fluopyram resistant isolates had the *sdh*C^{S105I} mutation in common and environmental boscalid resistant had the *sdh*B^{H270Y} mutation (Table 6).

3.3 Sexual Spore Crossing for Separating Resistance Conferring SNPs and Compensatory Mutations

To investigate the inheritance of alleles carrying the *sdh*C^{S105I} and *sdh*B^{H270Y} SNPs, as well as potential compensatory mutations, sexual crosses were performed between environmental resistant variants and high fertility strains of *A. fumigatus* (see Appendix 2). The progeny from these crosses exhibited morphological differences (Figure 4A-C), reflecting the segregation of alleles. Variations in growth patterns and sporulation were identified among sexual crosses between environmental resistant variants and high fertility sensitive strains.

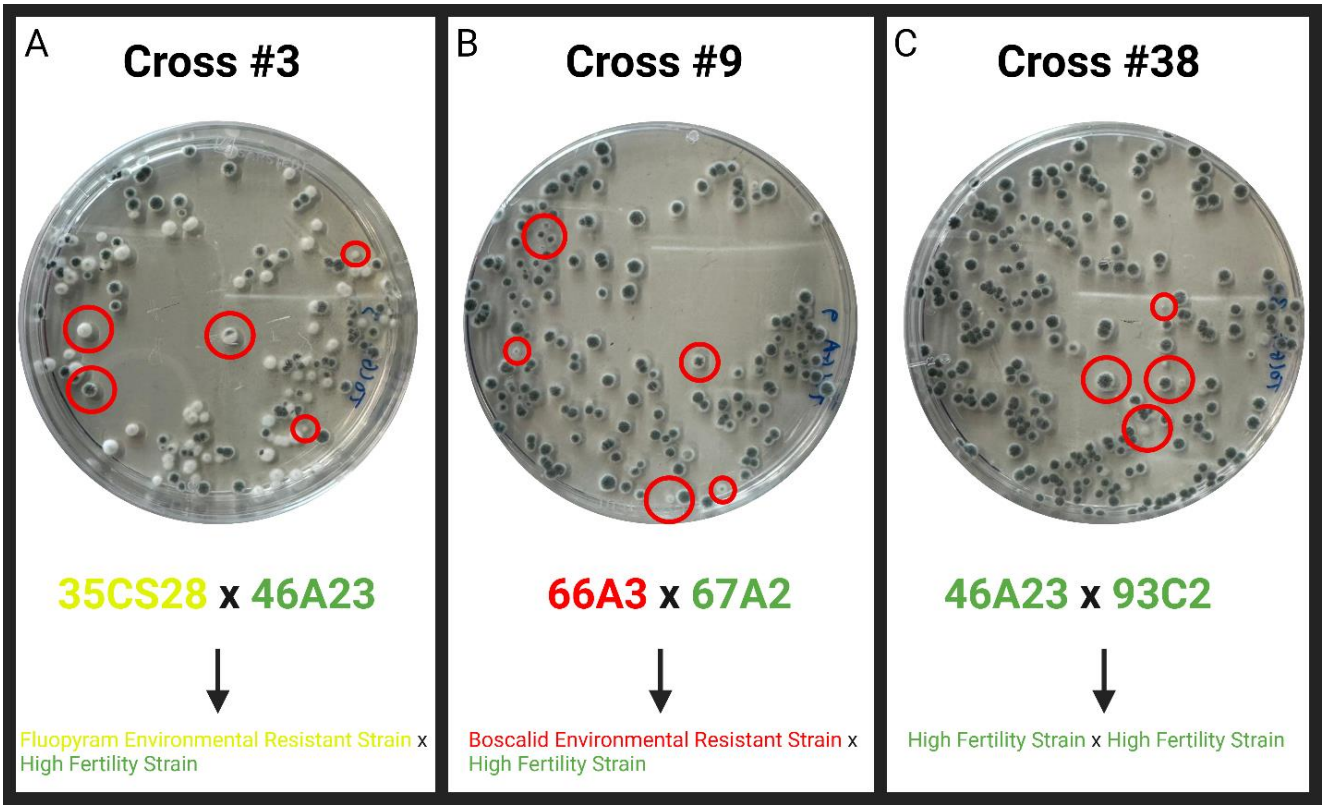

Figure 4 - Morphological differences in the progeny of crosses between environmental resistant strains and high fertility strains of *A. fumigatus*. Progeny marked with red circles include both those with defective growth and sporulation, as well as healthy ones, to facilitate comparison. Yellow indicates environmental fluopyram resistant variant, red indicates environmental boscalid variant, green indicates high fertility sensitive strains (see Appendix 2 for complete crossing list).

3.4 Inducing *sdh*C^{S105I} and *sdh*B^{H270Y} SNPs in AfiR974 High Fertility and Sensitive Strain for Fitness Assessments

CRISPR-Cas9-mediated mutagenesis was used to induce the *sdh*C^{S105I} SNP in the AfiR974 high fertility and sensitive strain. This mutation involved a guanine (G) to thymine (T) nucleotide substitution, resulting in the codon change and encoding of isoleucine (I) instead of serine (S) (Figure 5).

A similar approach was attempted for the *sdh*B^{H270Y} mutation. However, the CRISPR-Cas9-mediated mutagenesis was not sustained in the AfiR974 strain, and the sequence reverted to its original form. Before the reversion of *sdh*B^{H270Y} mutation, CRISPR-Cas9-mediated mutants

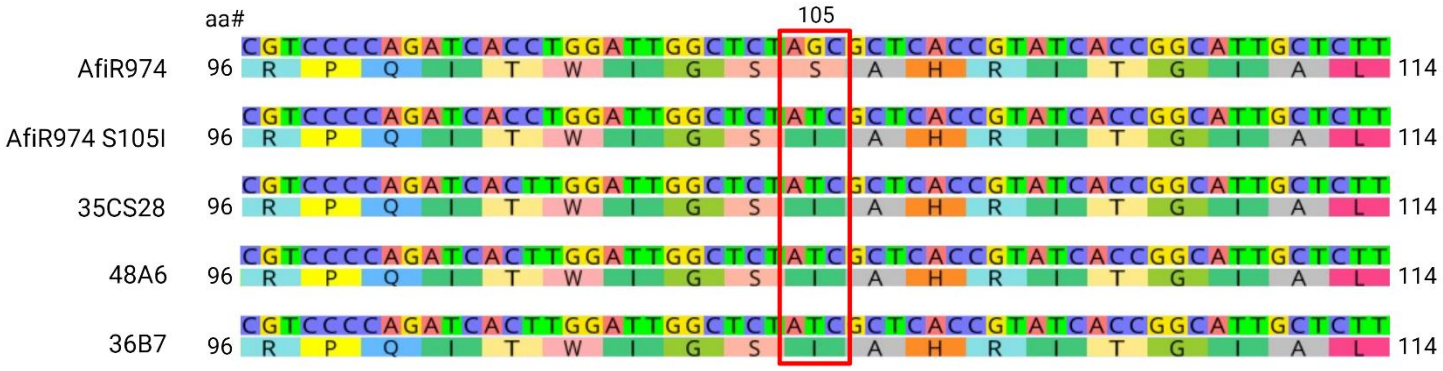

Figure 5 - Multiple Sequence Alignment of AfiR974, AfiR974 *sdh*C^{S105I} mutant, and environmental fluopyram resistant variants. The alignment highlights the CRISPR-Cas9 mediated mutagenesis at the 105th position in the *sdh*C gene, illustrating the amino acid substitution of serine to isoleucine due to a nucleotide change in the codon (AGC to ATC).

AfiR974 *sdh*C^{S105I} and AfiR974 *sdh*B^{H270Y} were tested under fluopyram and boscalid pressure, respectively, to confirm their resistance before proceeding with fitness assessments.

3.5 Impact of the *sdh*C^{S105I} Mutation on Fluopyram Binding and Alteration of SdhC Protein Interaction Sites

To evaluate the impact of the *sdh*C^{S105I} mutation on the docking of fluopyram to the SdhC protein subunit, 3D structures were simulated and docking analyses were performed. The amino

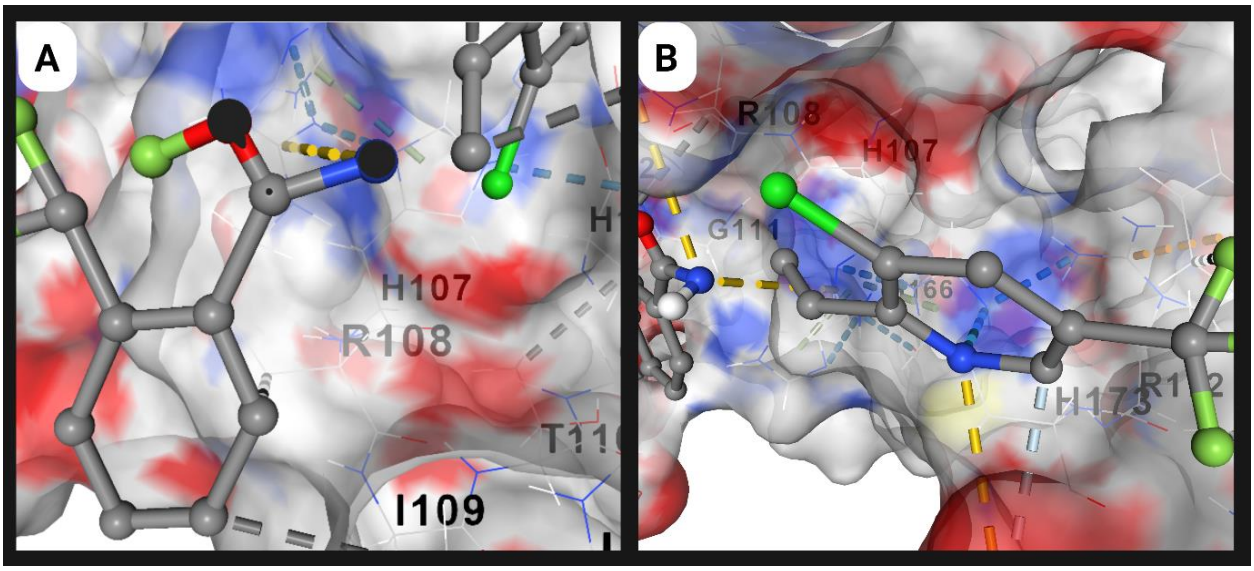

Figure 6 - 3D structure of fluopyram bound to the SdhC protein subunit. A, The displayed amino acid residues (H107, R108, I109) represent the specific regions involved in the interaction with fluopyram during binding in the AfiR974 high fertility and sensitive strain. **B,** This panel shows the predicted structure of the SdhC protein from the AfiR974 strain, incorporating the *sdh*C^{S105I} mutation. In this mutated structure, fluopyram no longer interacts with the isoleucine residue at position 109.

acid residues shown in the Figure 6A highlights the specific amino acid residues involved in the interactions between fluopyram and the SdhC protein. In Figure 6B, the 3D structure of the SdhC protein with the *sdh*C^{S105I} mutation demonstrates the loss of interaction with the isoleucine residue at position 109.

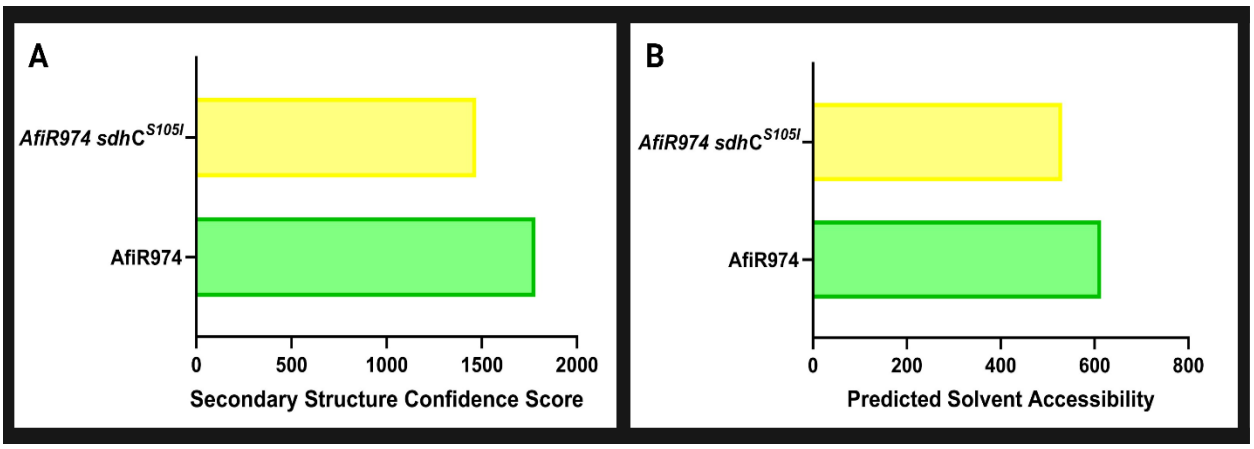

Figure 7 – Secondary structure confidence and solvent accessibility score changes in the SdhC protein of AfiR974 and the AfiR974 *sdh*C^{S105I} mutant.

From the 3D structure analysis, the secondary structure confidence score of the SdhC protein in the AfiR974 strain was 1782, while in the AfiR974 *sdh*C^{S105I} mutant, this score decreased to 1471, indicating a reduction in the confidence of the secondary structure (Figure 7A). A similar reduction is noted in the predicted solvent accessibility (Figure 7B). The solvent accessibility score for the SdhC protein in AfiR974 was 614, which decreased to 531 following the *sdh*C^{S105I} mutation (Figure 7B).

3.6 Fungal Burden Assay in *G. mellonella*

The survival rates of *G. mellonella* larvae infected with *A. fumigatus* environmental resistant variants were monitored over a seven-day period. During this period, the probability of survival of each treatment was assessed and plotted in Figure 8. The high fertility and sensitive strain AfiR974 caused complete mortality by day four, with 0% survival. Strain 11A6 demonstrated reduced virulence, with 55% survival by day seven. The environmental fluopyram resistant variant 35CS28 also led to 0% survival but required the full seven days, indicating a slower progression of infection compared to AfiR974. PBS and untreated larvae were included as controls.

The statistical comparison using the Log-rank (Mantel-Cox) test demonstrates a significant difference in virulence between the AfiR974 and the environmental boscalid resistant variant 11A6. The same test was applied to compare the virulence between AfiR974 and the fluopyram resistant variant 35CS28, revealing a significant difference as well.

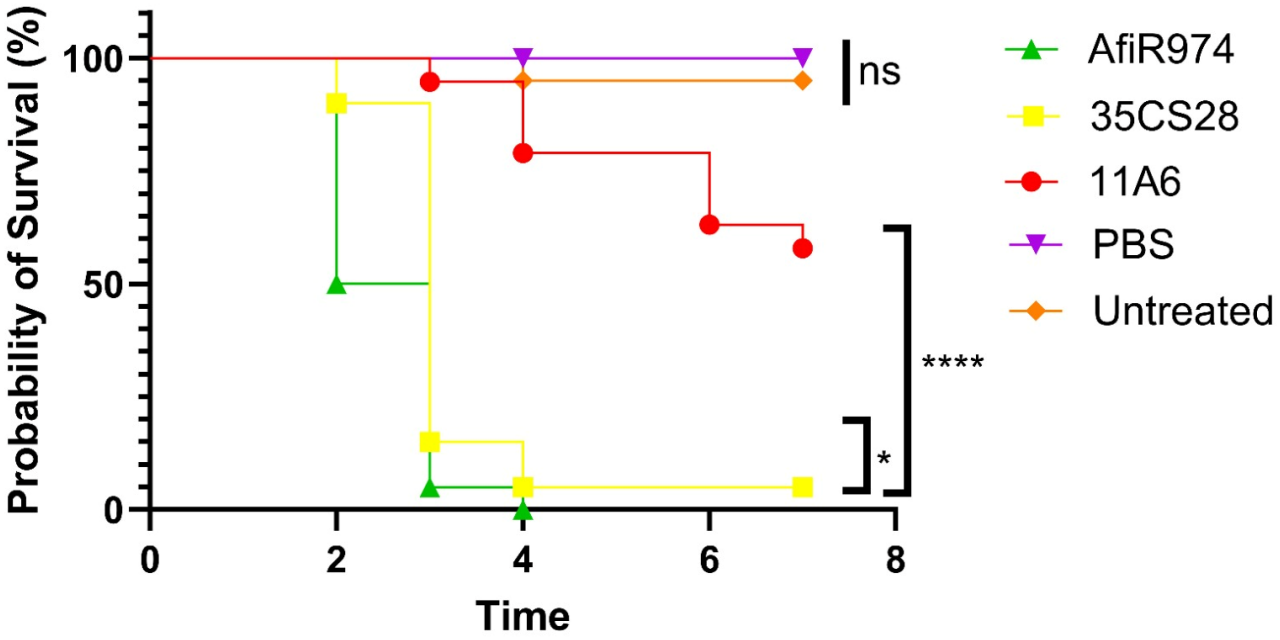

Figure 8 - Probability of survival of *G. mellonella* larvae over 7 days post-infection with *A. fumigatus* isolates. The comparison is based on the probability of survival (%) over days. The isolates include the environmental boscalid resistant variant (11A6), the environmental fluopyram resistant variant (35CS28), the high fertility and sensitive strain (AfiR974), and control groups (PBS and untreated larvae). An inoculum size of 1 x 10^5 spores per larvae was used for each treatment. The Log-rank (Mantel-Cox) test revealed significant differences in virulence between AfiR974 and 11A6 (****$p < 0.0001$) and between AfiR974 and 35CS28 (**$p = 0.0085$). Among the control groups, no statistically significant difference was observed (ns, $p = 0.3173$). ns = non-significant.

3.7 *sdh*C^{S105I} Mutation in AfiR974 Does Not Affect the Radial Growth

A radial growth assay was conducted to assess the fitness cost associated with the *sdh*C^{S105I} mutation compared to the high fertility and sensitive strain AfiR974. The AfiR974 *sdh*C^{S105I} showed reduced growth compared to AfiR974 over the three-day observation period (Figure 9). On day one, the AfiR974 *sdh*C^{S105I} mutant exhibited a mean radial growth of 5.9 mm, compared to AfiR974's 6.7 mm. By day two, the AfiR974 *sdh*C^{S105I} mutant reached 17.0 mm, while AfiR974 measured 17.9 mm. On day three, the maximum radial growth was recorded for 36B7 at 33.7 mm, with the AfiR974 *sdh*C^{S105I} mutant showing the lowest growth at 28.1 mm.

Despite the lack of statistically significant differences between the AfiR974 *sdh*C^{S105I} mutant and AfiR974, the mutant consistently demonstrated the lowest radial growth. The high fertility strains AfiR964 and AfiR974 showed similar growth patterns, while the environmental fluopyram resistant variant 48B6 nearly caught up with 35CS28 by day three. Statistical analysis

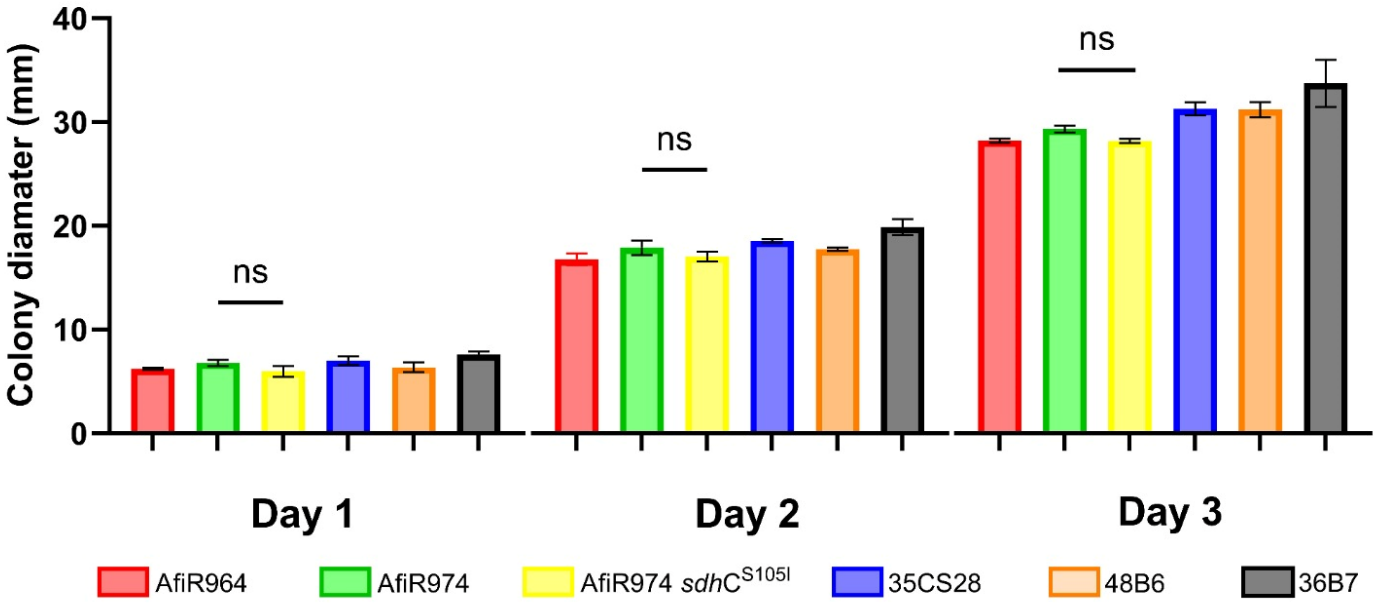

Figure 9 - Radial growth of *A. fumigatus* isolates over three days under normoxic conditions at 37°C. Comparison based on the colony diameter (mm) between the high fertility sensitive strains (AfiR964 and AfiR974), environmental fluopyram-resistant variants (35CS28, 48B6, and 36B7), and the AfiR974 *sdh*C^{S105I}mutant. The Welch's t-test did not reveal a significant difference between the AfiR974 and AfiR974 *sdh*C^{S105I} mutant ($p > 0.05$).

revealed no significant difference in radial growth between the AfiR974 and the AfiR974 *sdh*C^{S105I} mutant on each day of the experiment.

3.8 *sdh*C^{S105I} Mutation in AfiR974 Does Not Significantly Affect the Radial Growth Under Hypoxic Conditions

Another radial growth experiment was conducted under hypoxic conditions to assess the impact of *sdh*C^{S105I} mutation by comparing AfiR974 *sdh*C^{S105I} with AfiR974. On day one, AfiR974 showed a radial growth of 7.7 mm, while AfiR974 *sdh*C^{S105I} mutant showed 7.0 mm growth. This pattern continued on day two, with the AfiR974 *sdh*C^{S105I} mutant consistently showing less growth than the AfiR974 high fertility sensitive strain. By day three, 35CS28 demonstrated the highest radial growth, while AfiR964 had the least.

Under hypoxic conditions, the AfiR974 *sdh*C^{S105I} mutant exhibited a higher growth compared to normoxic conditions, nearly matching AfiR974's radial growth by the third day. Unlike the results under normoxic conditions (Figure 9), 36B7 did not show maximum growth, while 35CS28 demonstrated the highest growth under hypoxia (Figure 10). AfiR964 showed the lowest radial growth under both conditions (Figure 9 & 10). Statistical analysis revealed no significant difference in radial growth between the AfiR974 *sdh*C^{S105I} mutant and the AfiR974 high fertility and sensitive strain under hypoxic conditions.

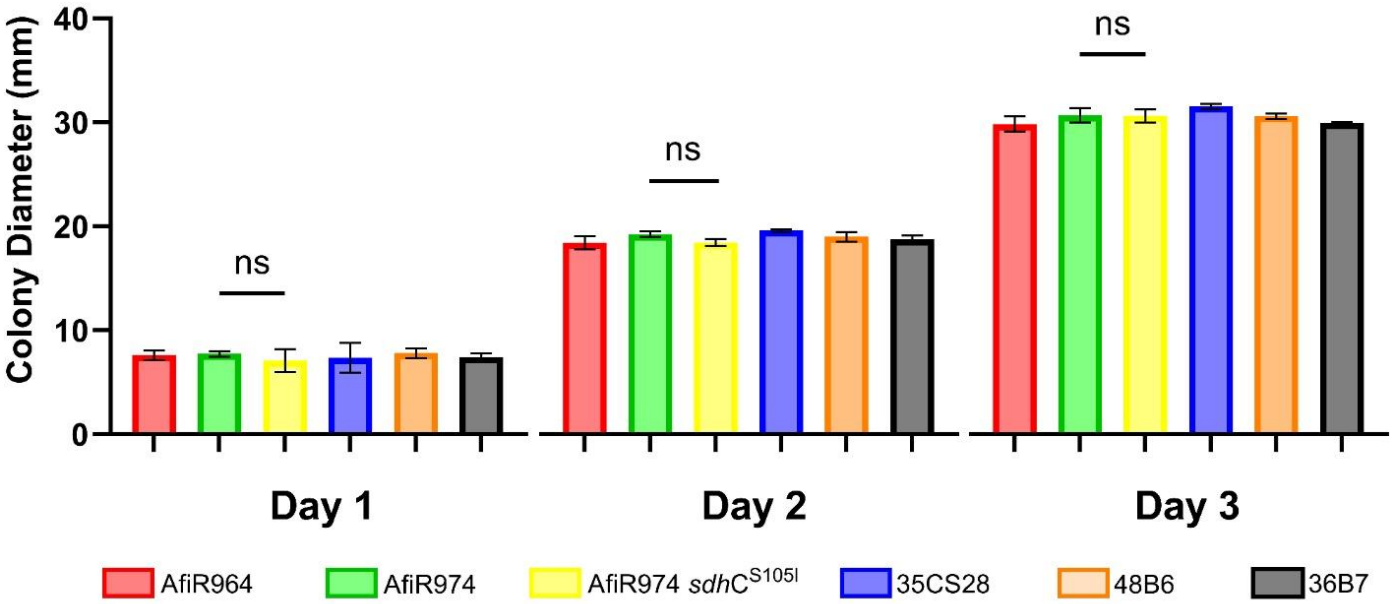

Figure 10 - Radial growth of *A. fumigatus* isolates under hypoxic conditions over three days at 37°C. Comparison based on the colony diameter (mm) between the high fertility sensitive strains (AfiR964 and AfiR974), environmental fluopyram resistant variants (35CS28, 48B6, and 36B7), and the AfiR974 *sdh*C^{S105I} mutant. The Welch's t-test did not reveal a significant difference between the AfiR974 and AfiR974 *sdh*C^{S105I} mutant ($p > 0.05$).

3.9 *sdh*C^{S105I} Mutation in AfiR974 Has No Role in Altering Fungal Biomass Production

Fungal biomass production was assessed after four days of incubation to evaluate any fitness costs associated with the *sdh*C^{S105I} mutation. The environmental fluopyram resistant variant 48A6 showed the highest biomass production across all tested strains (Figure 11). Both the AfiR974 *sdh*C^{S105I} mutant and the environmental fluopyram resistant variant 35CS28 produced similar levels of biomass.

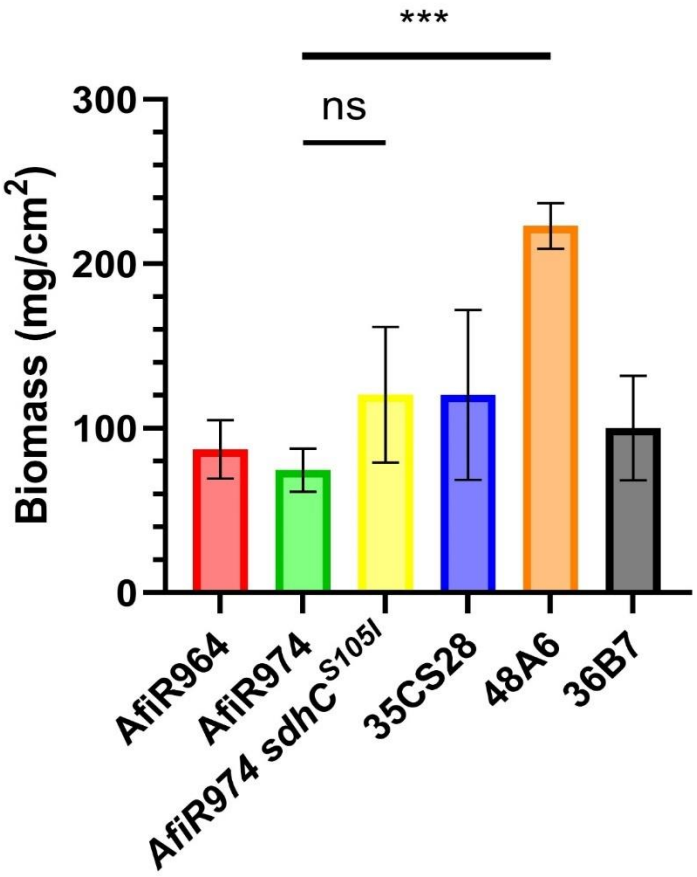

Figure 11 – Dry biomass production of *A. fumigatus* isolates after 4 days of incubation at 37°C. Comparison of dry fungal biomass (mg/cm^2) between high fertility sensitive strains (AfiR964 and AfiR974), the AfiR974 *sdh*C^{S105I} mutant, and environmental fluopyram resistant variants (35CS28, 48A6, and 36B7). The Welch's t-test revealed a significant difference between the environmental fluopyram resistant strain 48A6 and AfiR974 (***p- value = 0.0002). However, no statistically significant difference was observed in biomass production between the AfiR974 *sdhC* ^{S105I} mutant and AfiR974 ($p > 0.05$).

The high fertility strains AfiR964 and AfiR974 showed comparable biomass production, similar to 36B7. Although there were no significant differences between the high fertility strains (AfiR964 and AfiR974) and the AfiR974 *sdh*C^{S105I} mutant, the overall trend suggested that the AfiR974 *sdh*C^{S105I} mutant produced more biomass than the AfiR974 strain, but this difference was not statistically significant.

4. Discussion

4.1 Idenification of Mutations that Select for Resistance to SDHIs in Environmental *A. fumigatus* Isolates

Mutations selecting resistance to fluopyram and boscalid in fungal plant pathogens which often come with fitness costs, have been identified and studied in previous publications (Amiri et al., 2020). Despite advances in understanding SDHI resistance in fungal plant pathogens, a significant knowledge gap persists regarding the resistance mechanisms of *A. fumigatus* in environmental settings. This gap extends to understanding the mechanisms and impacts of SDHI resistance, mutations selecting for resistance, associated fitness costs, and potential compensatory mutations that mitigate these costs, especially since the environmental isolates studied have been competing and surviving over multiple generations. To address these knowledge gaps, we assessed the 84 environmental *A. fumigatus* isolates from the Netherlands using boscalid and fluopyram. While previous studies on fungal plant pathogens utilized boscalid and fluopyram alongside other SDHIs to broaden the analysis of resistance mechanisms (Miyamoto et al., 2020), our assessment specifically demonstrated a clear frequency of resistant variants within a small population. Although this frequency, 8.33% fluopyram resistant and 2.38% boscalid resistant, does not reflect the overall likelihood of resistant variants, it provides insight into their distribution. Within the 84 environmental *A. fumigatus* isolates (see Appendix 1), we identified the mutations *sdh*C^{S105I} in *sdh*C gene and *sdh*B^{H270Y} in *sdh*B gene, which confer resistance to fluopyram and boscalid, respectively. These mutations are in the highly conserved SdhC and SdhB subunits of the SDH complex, which plays a crucial role in cellular respiration (Bénit et al., 2019). The nucleotide changes from these mutations resulted in amino acid substitutions, leading to further investigation into the mutations and their effects on fitness.

4.2 Potential Effects of *sdh*C^{S105I} and *sdh*B^{H270Y} Mutations in Environmental Resistant Variants

To further investigate, we conducted sexual crossing experiments to separate alleles carrying the *sdh*C^{S105I} and *sdh*B^{H270Y} mutations that select for resistance from potential compensatory mutations. Despite harboring the *sdh*C^{S105I} and *sdh*B^{H270Y} mutations, which confer resistance to fluopyram and boscalid, the environmental resistant variants exhibited growth rates similar to those of environmental SDHI-sensitive strains. This suggests the potential presence of compensatory mutations that mitigate the fitness costs that are associated with the *sdh*C^{S105I} and *sdh*B^{H270Y} mutations, allowing the resistant variants to maintain competitive growth over generations under no SDHI pressure. Sexual crossings between environmental resistant variants and high fertility SDHI-sensitive strains revealed defective offspring, suggesting that the resistance mutation was inherited without the compensatory mutation, likely due to the high number of meiotic crossovers (Auxier et al., 2023). This points to the presence of fitness costs associated with the *sdh*C^{S105I} and *sdh*B^{H270Y} mutations. However, it is important to note that the background of the environmental resistant variants may include exposure to other fungicides, which could influence

resistance patterns (Kang et al., 2022). As a result, the defective progeny might result from another resistance mechanism to fungicides not identified in this study. Additionally, the presence of epistatic genes, which can influence the expression of other genes, might mask the effects of hypostatic genes, potentially effecting critical traits beyond those linked to resistance (Pérez-Pérez et al., 2009).

Building upon this foundation, a virulence assay was conducted in this study *using G. mellonella* infection model to determine whether the environmental resistant variants exhibit different virulence profiles (Macdonald et al., 2019) compared to the high fertility and SDHI-resistant strain, AfiR974. Our results indicated that the environmental resistant variants have reduced pathogenicity compared to AfiR974, supporting the presence of fitness costs. This result aligns with other studies demonstrating that hyphal growth is essential for invading and destroying host tissue to obtain nutrients, directly linking it to virulence (Paulussen et al., 2017). Our data suggests that the reduced pathogenicity observed in the environmental resistant variants may be due to the *sdh*C^{S105I} and *sdh*B^{H270Y} mutations. These mutations likely alter hyphal production, potentially impairing the ability to invade host tissue and reducing its virulence.

Due to the suggestive data, this study proceeded by specifically assessing the effects of the *sdh*C^{S105I} and *sdh*B^{H270Y} mutations. However, evaluating the direct effects of the *sdh*C^{S105I} and *sdh*B^{H270Y} mutations in environmental resistant variants can be misleading due to variations in their genetic backgrounds (Alshareef & Robson, 2014), which may include compensatory mutations. To eliminate this variable, we induced the *sdh*C^{S105I} and *sdh*B^{H270Y} mutations in the genetic background of AfiR974. However, during the single-spore purification step, the induced *sdh*B^{H270Y} mutation in AfiR974 was not detectable in the *sdh*B gene, pointing to a severe fitness cost associated with this mutation. As demonstrated by Claus et al. (2022), in fungi, when a mutation has deleterious or lethal characteristics, maintaining a functional wild-type nucleus is considered as a survival strategy to prevent fitness penalties in the absence of selection pressure. Consequently, only the *sdh*C^{S105I} mutation was successfully induced.

4.3 Fitness Assessments Revealed No Fitness Costs Associated with *sdh*C^{S105I} Mutation

After inducing the *sdh*C^{S105I} in the high fertility and SDHI-sensitive AfiR974 strain, this study focused on exploring the fitness costs. In other studies, experiments such as osmotic and oxidative stress tests (Veloukas et al., 2014), germination assays (Sun et al., 2021), radial growth measurements (Piotrowska et al., 2017), and dry biomass production (Li et al., 2022) are conducted to identify mutations' effects on crucial cellular mechanisms. Considering the location where the *sdh*C^{S105I} mutation occurs, the radial growth under normoxic and hypoxic conditions and dry fungal biomass analyses were selected to assess the effects of the *sdh*C^{S105I} mutation by measuring the fungal colony expansion on solid media and quantifying the total fungal material in liquid culture. The results showed that the AfiR974 *sdh*C^{S105I} mutant is not defective in radial growth under normoxic and hypoxic conditions and dry biomass production. This observation correlates with the mutation's frequency within the population of 84 environmental isolates (8.33%),

suggesting that if the *sdh*C^{S105I} mutation incurred significant fitness costs, it would not be maintained over generations in an environment without SDHI pressure. However, the finding that *sdh*C^{S105I} mutation does not lead to a fitness cost is contradictory to the fungal burden assay, which suggested a fitness cost associated with the *sdh*C^{S105I} mutation. But since it is proven that the *sdh*C^{S105I} mutation not being associated with a fitness cost, the differences in virulence between 35CS28 and AfiR974 are estimated to be due to their genetic backgrounds. Additionally, the *sdh*B^{H270Y} mutation's lower frequency (2.38%) within the population of 84 environmental isolates (see Appendix 1) supports the notion that it is associated with substantial fitness costs.

Comparing our results with other studies, the *sdh*C^{I86F} amino acid substitution in the SdhC protein (Claus et al., 2022) and the *sdh*B^{H278Y} substitution in the SdhB protein (Shi et al., 2021) have been linked to fitness costs in *Corynespora cassiicola* and *Phakopsora pachyrhizi*, respectively. These include reduced mycelial growth and increased sensitivity to osmotic and oxidative stress. Given that the *sdh*B^{H278Y} mutation in *P. pachyrhizi* is located in close proximity to the *sdh*B^{H270Y} mutation, we anticipate it will exhibit similar fitness costs due to their spatial closeness within the gene. In contrast, the *sdh*C^{I86F} mutation in *C. cassicola*, which is not closely positioned to *sdh*C^{S105I} mutation, do not share the similar effect in terms of fitness cost. Indeed, the population frequency of the *sdh*C^{I86F} mutation in *C. cassicola* increased from 7% to 48% over four years in Brazil, indicating that this mutation can be stable over generations and become prevalent in populations (Claus et al., 2022). Conversely, the *sdh*B^{H278Y} mutation in *P. pachyrhizi* showed a different pattern; while most strains in Shandong and Liaoning provinces carried the *sdh*B^{H278Y} mutation in 2014, it was not detected in 2018 and 2019 (Shi et al., 2021). This change can be explained by the fungus' survival mechanism of maintaining a wild-type nucleus without mutations that incur fitness costs (Simões et al., 2018).

4.4 Future Recommendations

With the current results, this study could not address the presence of compensatory mutations in detail. However, the sexual crossing experiment suggests that compensatory mutations for the *sdh*B^{H270Y} mutation may be present. Future studies can build upon this by performing bulk segregation analyses to examine the genetic backgrounds of defective and healthy progeny. Since BSA has been used to identify the genetic basis of specific traits or mutations, compensatory mutations can be identified by creating bulks (Shen & Messer, 2022). This involves pooling together groups of defective and healthy progeny, followed by sequencing analysis to reveal the mutations of interest (Ashton et al., 2022). This way, sequencing results can help identify the compensatory mutations, which should then be introduced into strains that only carry the CRISPR-Cas9 mediated resistance mutation associated with a fitness cost for confirmation. Another aspect for future research is to assess different SDHIs used in agriculture, such as penthiopyrad and isopyrazam, to identify different mutations that might select for resistance to these newer SDHIs. Mutations that select for resistance to SDHIs can be assessed for fitness costs using various experimental setups, including oxidative and osmotic stress tests, fungal burden assays, sporulation rate measurements, and competition assays using grass as a substrate to

compete different strains. Instead of using plates and minimal media to conduct competition assays under laboratory conditions (Neher & Weicht, 2018), grass is used as a carbon source (Rhodes, 2006), with PBS added as a moisture source to better simulate natural environmental conditions (Delabona et al., 2013). The inoculation of different strains triggers antagonistic activity, leading to competition for resources (Delabona et al., 2013). The outcome of this assay is analyzed by collecting mixed spores and calculating a ratio based on the allelic differences among the strains (Zulak et al., 2024). This approach enables the observation of the relative dominance of each isolate, indicating which strain is more competitive based on the proportion of allele reads.

4.5 Conclusion

In conclusion, this study identified and highlighted the mechanism of boscalid and fluopyram resistance by detecting the *sdh*B^{H270Y} and *sdh*C^{S105I} mutations, which are responsible for selecting for resistance to boscalid and fluopyram, respectively. Additionally, the study predicted the 3D structure of the SdhC protein and analyzed the binding pattern of fluopyram before and after the *sdh*C^{S105I} mutation, which causes the substitution of serine with isoleucine. This mutation is predicted to alter the structure of the SdhC protein by lowering the secondary structure confidence score and predicted solvent accessibility, contributing to fluopyram resistance.

Furthermore, the boscalid and fluopyram sensitivity testing of 84 environmental *A. fumigatus* isolates led to the identification of resistant variants. To assess whether these environmental resistant variants carry any fitness costs, sexual crossing and fungal burden experiments were performed. These experiments suggested the presence of fitness costs and potential compensatory mutations associated with the *sdh*B^{H270Y} and *sdh*C^{S105I} mutations. However, while this study explored fitness costs, it was only able to specifically assess the effect of the *sdh*C^{S105I} mutation by introducing it into the AfiR974 background and testing radial growth rates under normoxic and hypoxic conditions, as well as dry fungal biomass production. The *sdh*B^{H270Y} mutation could not be tested for fitness cost in this study.

The results demonstrated that the *sdh*C^{S105I} mutation is not associated with a fitness cost in *A. fumigatus*, and as a result, no compensatory mutations were identified for this mutation. In contrast, the *sdh*B^{H270Y} mutation appeared to be linked to fitness costs, suggesting the possibility of compensatory mutations that mitigate these effects. Through these findings, this study significantly contributes to filling the knowledge gap regarding the mechanisms and impacts of SDHI resistance in *A. fumigatus*.

5. Appendix

Appendix 1: Table showing the 84 environmental isolates with reference numbers and sample IDs.

Reference Number	Sample ID
1	27C10
2	27C7
3	26BS
4	95C20
5	19B4
6	18A3
7	18A1
8	16C32
9	39B10
10	46A8
11	63C6
12	5A16
13	56C17
14	94B6
15	55C3
16	59B4
17	50C32
18	47A8
19	66A16
20	67A3
21	77B14
22	99B16
23	98C12
24	81C3
25	74C8
26	79A19
27	68A13
28	56C20
29	50C32
30	67A2
31	10C11
32	29C8
33	96C24
34	40A21
35	48A6
36	48A5
37	36B7
38	76A18
39	11A6
40	13B9
41	18A2
42	13B11
43	67A5
44	33MKI
45	35CS28
46	66A3
47	AfiR974
48	78C2
49	55C4
50	88C20
51	4A19
52	82C23
53	9C23
54	46A23
55	72A6
56	69A4
57	55C1
58	4A18
59	48A4
60	40A20
61	38C31
62	34BO24
63	11A2
64	9C22
65	86C22
66	85C12
67	84C7
68	83C13
69	82C21
70	91C14
71	8-C17
72	79C1
73	78C1
74	76A17
75	87C25
76	8C2
77	72A8
78	58C25
79	98C11
80	96C26
81	95A8
82	93C2
83	88C19
84	11A5

Appendix 2: Sexual crossing map for the crossing experiment. The map was designed using 5 MAT 1-1 high fertility and sensitive strains (46A23, 67A2, AfiR974, AfiR957, AFRB2), 4 MAT 1-2 high fertility and sensitive strains (93C2, AfiR964, AfiR928, AfiR956), 3 MAT 1-1 resistant variants (48A6, 76A18, 36B7), and 5 MAT 1-2 resistant variant strains (48A5, 11A6, 35CS28, 66A3, 78C2). T HF = high fertility, RV = resistant variant.

Number	MAT 1-1 HF	MAT 1-2 RV
1	46A23	48A5
2	46A23	11A6
3	46A23	35CS28
4	46A23	66A3
5	46A23	78C2
6	67A2	48A5
7	67A2	11A6
8	67A2	35CS28
9	67A2	66A3
10	67A2	78C2
11	AfiR974	48A5
12	AfiR974	11A6
13	AfiR974	35CS28
14	AfiR974	66A3
15	AfiR974	78C2
16	AfiR957	48A5
17	AfiR957	11A6
18	AfiR957	35CS28
19	AfiR957	66A3
20	AfiR957	78C2
21	AfiRB2	48A5
22	AfiRB2	11A6
23	AfiRB2	35CS28
24	AfiRB2	66A3
25	AfiRB2	78C2

Table 7A – Crossing map for environmental resistant variants.

Number	MAT 1-2 HF	MAT 1-1 RV
26	93C2	48A6
27	93C2	36B7
28	93C2	76A18
29	AfIR964	48A6
30	AfIR964	36B7
31	AfIR964	76A18
32	AfIR928	48A6
33	AfIR928	36B7
34	AfIR928	76A18
35	AfIR956	48A6
36	AfIR956	36B7
37	AfIR956	76A18

Table 7B – Crossing map for environmental resistant variants.

Number	MAT 1-2 HF	MAT 1-1 HF
38	93C2	48A23
39	93C2	67A2
40	93C2	AfiR974
41	93C2	AfiR957
42	93C2	AFRB2
43	AfiR964	48A23
44	AfiR964	67A2
45	AfiR964	AfiR974
46	AfiR964	AfiR957
47	AfiR964	AFRB2
48	AfiR928	48A23
49	AfiR928	67A2
50	AfiR928	AfiR974
51	AfiR928	AfiR957
52	AfiR928	AFRB2
53	AfiR956	48A23
54	AfiR956	67A2
55	AfiR956	AfiR974
56	AfiR956	AfiR957
57	AfiR956	AFRB2

Table 7C – Crossing map for positive control.

Number	MAT 1-1 RV	MAT 1-2 RV
58	48A6	48A5
59	48A6	11A6
60	48A6	35CS28
61	48A6	66A3
62	48A6	78C2
63	76A18	48A5
64	76A18	11A6
65	76A18	35CS28
66	76A18	66A3
67	76A18	78C2
68	36B7	48A5
69	36B7	11A6
70	36B7	35CS28
71	36B7	66A3
72	36B7	78C2
73	48A6	48A6
74	76A18	76A18
75	36B7	36B7
76	48A5	48A5
77	11A6	11A6
78	35CS28	35CS28
79	66A3	66A3
80	78C2	78C2

Table 7D – Crossing map for negative control.

Appendix 3: Diagram showing the inoculation locations for the sexual crossing experiment between two strains.

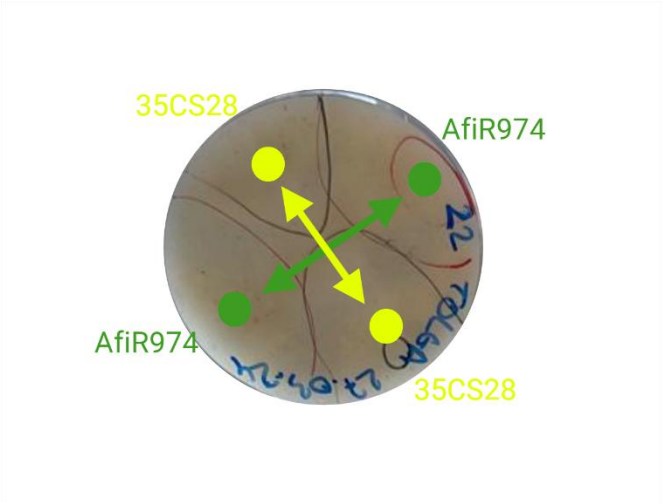

Appendix 4: Amino acid sequences of SdhC protein from AfiR974 and AfiR974 *sdh*C^{S105I} mutant used in 3D structure analysis and SdhC protein-fluopyram binding simulations.

SdhC Amino Acid Sequence	
AfiR974	AfiR974 *sdh*C^{S105I} Mutant
MISQKVAQQSLRRRMYSPACCLICLSRLT NNPAVAVQQPYAMRWSLMNSASPAAVA MGRNVQKRHAASTTSQADASKILAQQR LNRPVSPHLSIYRPQITWIGSSAHRITGIA LSGSLYLFATAYLAAPLFGWHLESASIAA AFGALPIAAKVLIKGTAAFPFVYHCLNG VRHLVWDLGRGISNQQVIKSGWTVVGL TVVSALTLALL	MISQKVAQQSLRRRMYSPACCLICLSRLT NNPAVAVQQPYAMRWSLMNSASPAAVA MGRNVQKRHAASTTSQADASKILAQQR LNRPVSPHLSIYRPQITWIGSIAHRITGIAL SGSLYLFATAYLAAPLFGWHLESASIAAA FGALPIAAKVLIKGTAAFPFVYHCLNGV RHLVWDLGRGISNQQVIKSGWTVVGLT VVSALTLALL

6. References

Alshareef, F., & Robson, G. D. (2014). Genetic and virulence variation in an environmental population of the opportunistic pathogen Aspergillus fumigatus. *Microbiology (United Kingdom)*, *160*(PART 4). https://doi.org/10.1099/mic.0.072520-0

Amiri, A., Zuniga, A. I., & Peres, N. A. (2020). Mutations in the membrane-anchored SdhC subunit affect fitness and sensitivity to succinate dehydrogenase inhibitors in botrytis cinerea populations from multiple hosts. *Phytopathology*, *110*(2), 327–335. https://doi.org/10.1094/PHYTO-07-19-0240-R

Ashton, G. D., Sang, F., Blythe, M., Zadik, D., Holmes, N., Malla, S., Camps, S. M. T., Wright, V., Melchers, W. J. G., Verweij, P. E., & Dyer, P. S. (2022). Use of Bulk Segregant Analysis for Determining the Genetic Basis of Azole Resistance in the Opportunistic Pathogen Aspergillus fumigatus. *Frontiers in Cellular and Infection Microbiology*, *12*. https://doi.org/10.3389/fcimb.2022.841138

Auxier, B., Debets, A. J. M., Stanford, F. A., Rhodes, J., Becker, F. M., Marquez, F. R., Nijland, R., Dyer, P. S., Fisher, M. C., den Heuvel, J. van, & Snelders, E. (2023). The human fungal pathogen Aspergillus fumigatus can produce the highest known number of meiotic crossovers. *PLoS Biology*, *21*(9 September). https://doi.org/10.1371/journal.pbio.3002278

Avenot, H. F., & Michailides, T. J. (2010). Progress in understanding molecular mechanisms and evolution of resistance to succinate dehydrogenase inhibiting (SDHI) fungicides in phytopathogenic fungi. In *Crop Protection* (Vol. 29, Issue 7, pp. 643–651). https://doi.org/10.1016/j.cropro.2010.02.019

Awuchi, C. G., Ondari, E. N., Nwozo, S., Odongo, G. A., Eseoghene, I. J., Twinomuhwezi, H., Ogbonna, C. U., Upadhyay, A. K., Adeleye, A. O., & Okpala, C. O. R. (2022). Mycotoxins' Toxicological Mechanisms Involving Humans, Livestock and Their Associated Health Concerns: A Review. *Toxins*, *14*(3). https://doi.org/10.3390/TOXINS14030167

Bénit, P., Kahn, A., Chretien, D., Bortoli, S., Huc, L., Schiff, M., Gimenez-Roqueplo, A. P., Favier, J., Gressens, P., Rak, M., & Rustin, P. (2019). Evolutionarily conserved susceptibility of the mitochondrial respiratory chain to SDHI pesticides and its consequence on the impact of SDHIs on human cultured cells. *PLoS ONE*, *14*(11). https://doi.org/10.1371/journal.pone.0224132

Berger, S., Chazli, Y. El, Babu, A. F., & Coste, A. T. (2017). Azole resistance in Aspergillus fumigatus: A consequence of antifungal use in agriculture? In *Frontiers in Microbiology* (Vol. 8, Issue JUN). Frontiers Media S.A. https://doi.org/10.3389/fmicb.2017.01024

Brauer, V. S., Rezende, C. P., Pessoni, A. M., De Paula, R. G., Rangappa, K. S., Nayaka, S. C., Gupta, V. K., & Almeida, F. (2019). Antifungal agents in agriculture: Friends and foes of public health. In *Biomolecules* (Vol. 9, Issue 10). https://doi.org/10.3390/biom9100521

Camps, S. M. T., Van Der Linden, J. W. M., Li, Y., Kuijper, E. J., Van Dissel, J. T., Verweij, P. E., & Melchers, W. J. G. (2012). Rapid induction of multiple resistance mechanisms in

Aspergillus fumigatus during azole therapy: A case study and review of the literature. *Antimicrobial Agents and Chemotherapy*, *56*(1), 10–16. https://doi.org/10.1128/AAC.05088-11

Claus, A., Simões, K., & May De Mio, L. L. (2022). Sdh C-I86F Mutation in Phakopsora pachyrhizi Is Stable and Can Be Related to Fitness Penalties. *Phytopathology*, *112*(7). https://doi.org/10.1094/PHYTO-10-21-0419-R

Delabona, P. da S., Pirota, R. D. P. B., Codima, C. A., Tremacoldi, C. R., Rodrigues, A., & Farinas, C. S. (2013). Effect of initial moisture content on two Amazon rainforest Aspergillus strains cultivated on agro-industrial residues: Biomass-degrading enzymes production and characterization. *Industrial Crops and Products*, *42*(1). https://doi.org/10.1016/j.indcrop.2012.05.035

Dzhavakhiya, V., Shcherbakova, L., Semina, Y., Zhemchuzhina, N., & Campbell, B. (2012). Chemosensitization of plant pathogenic fungi to agricultural fungicides. *Frontiers in Microbiology*, *3*(MAR). https://doi.org/10.3389/fmicb.2012.00087

Engle, K., & Kumar, G. (2024). Tackling multi-drug resistant fungi by efflux pump inhibitors. In *Biochemical Pharmacology* (Vol. 226). Elsevier Inc. https://doi.org/10.1016/j.bcp.2024.116400

Fraczek, M. G., Zhao, C., Dineen, L., Lebedinec, R., Bowyer, P., Bromley, M., & Delneri, D. (2019). Fast and Reliable PCR Amplification from Aspergillus fumigatus Spore Suspension Without Traditional DNA Extraction. *Current Protocols in Microbiology*, *54*(1). https://doi.org/10.1002/cpmc.89

Gonzalez-Jimenez, I., Garcia-Rubio, R., Monzon, S., Lucio, J., Cuesta, I., & Mellado, E. (2021). *Multiresistance to Nonazole Fungicides in Aspergillus fumigatus TR 34 /L98H Azole-Resistant Isolates*. https://journals.asm.org/journal/aac

Hawkins, N. J., & Fraaije, B. A. (2018). *Annual Review of Phytopathology Fitness Penalties in the Evolution of Fungicide Resistance*. https://doi.org/10.1146/annurev-phyto-080417

Hearn, V. M., Wilson, E. V, & R Mackenzie, D. W. (1980). THE PREPARATION OF PROTOPLASTS FROM ASPERGILLUS FUMIGATUS MYCELIUM. In *Sabouraudia* (Vol. 18).

Her, Y. F., & Maher, L. J. (2015). Succinate dehydrogenase loss in familial paraganglioma: Biochemistry, genetics, and epigenetics. In *International Journal of Endocrinology* (Vol. 2015). Hindawi Publishing Corporation. https://doi.org/10.1155/2015/296167

Hof, H. (2001). Critical Annotations to the Use of Azole Antifungals for Plant Protection. *Antimicrobial Agents and Chemotherapy*, *45*(11), 2987. https://doi.org/10.1128/AAC.45.11.2987-2990.2001

Howard, S. J., Webster, I., Moore, C. B., Gardiner, R. E., Park, S., Perlin, D. S., & Denning, D. W. (2006). Multi-azole resistance in Aspergillus fumigatus. *International Journal of Antimicrobial Agents*, *28*(5). https://doi.org/10.1016/j.ijantimicag.2006.08.017

Hu, M., & Chen, S. (2021). Non-target site mechanisms of fungicide resistance in crop pathogens: A review. In *Microorganisms* (Vol. 9, Issue 3). https://doi.org/10.3390/microorganisms9030502

Jampilek, J. (2016). Potential of agricultural fungicides for antifungal drug discovery. In *Expert Opinion on Drug Discovery* (Vol. 11, Issue 1). https://doi.org/10.1517/17460441.2016.1110142

Jørgensen, L. N., & Heick, T. M. (2021). Azole Use in Agriculture, Horticulture, and Wood Preservation – Is It Indispensable? *Frontiers in Cellular and Infection Microbiology*, *11*, 730297. https://doi.org/10.3389/FCIMB.2021.730297/BIBTEX

Kang, S. E., Sumabat, L. G., Melie, T., Mangum, B., Momany, M., & Brewer, M. T. (2022). Evidence for the agricultural origin of resistance to multiple antimicrobials in Aspergillus fumigatus, a fungal pathogen of humans. *G3 (Bethesda, Md.)*, *12*(2). https://doi.org/10.1093/g3journal/jkab427

Lalève, A., Fillinger, S., & Walker, A. S. (2014). Fitness measurement reveals contrasting costs in homologous recombinant mutants of Botrytis cinerea resistant to succinate dehydrogenase inhibitors. *Fungal Genetics and Biology*, *67*, 24–36. https://doi.org/10.1016/j.fgb.2014.03.006

Leroux, P., Gredt, M., Leroch, M., & Walker, A. S. (2010). Exploring mechanisms of resistance to respiratory inhibitors in field strains of botrytis cinerea, the causal agent of gray mold. *Applied and Environmental Microbiology*, *76*(19), 6615–6630. https://doi.org/10.1128/AEM.00931-10

Li, X., Gao, X., Hu, S., Hao, X., Li, G., Chen, Y., Liu, Z., Li, Y., Miao, J., Gu, B., & Liu, X. (2022). Resistance to pydiflumetofen in Botrytis cinerea: risk assessment and detection of point mutations in sdh genes that confer resistance. *Pest Management Science*, *78*(4), 1448–1456. https://doi.org/10.1002/ps.6762

Liu, Y., Grimm, M., Dai, W. tao, Hou, M. chun, Xiao, Z. X., & Cao, Y. (2020). CB-Dock: a web server for cavity detection-guided protein–ligand blind docking. *Acta Pharmacologica Sinica*, *41*(1), 138–144. https://doi.org/10.1038/s41401-019-0228-6

Macdonald, D., Thomson, D. D., Johns, A., Valenzuela, A. C., Gilsenan, J. M., Lord, K. M., Bowyer, P., Denning, D. W., Read, N. D., & Bromley, M. J. (2019). Inducible cell fusion permits use of competitive fitness profiling in the human pathogenic fungus aspergillus fumigatus. *Antimicrobial Agents and Chemotherapy*, *63*(1). https://doi.org/10.1128/AAC.01615-18

Miyamoto, T., Hayashi, K., Okada, R., Wari, D., & Ogawara, T. (2020). Resistance to succinate dehydrogenase inhibitors in field isolates of Podosphaera xanthii on cucumber: Monitoring,

cross-resistance patterns and molecular characterization. *Pesticide Biochemistry and Physiology*, *169*. https://doi.org/10.1016/j.pestbp.2020.104646

Miyamoto, T., Ishii, H., & Tomita, Y. (2010). Occurrence of boscalid resistance in cucumber powdery mildew in Japan and molecular characterization of the iron-sulfur protein of succinate dehydrogenase of the causal fungus. *Journal of General Plant Pathology*, *76*(4), 261–267. https://doi.org/10.1007/s10327-010-0248-z

Neher, D. A., & Weicht, T. R. (2018). A Plate Competition Assay As a Quick Preliminary Assessment of Disease Suppression. *Journal of Visualized Experiments : JoVE*, *140*. https://doi.org/10.3791/58767

Nywening, A. V., Rybak, J. M., Rogers, P. D., & Fortwendel, J. R. (2020). Mechanisms of triazole resistance in Aspergillus fumigatus. In *Environmental Microbiology* (Vol. 22, Issue 12, pp. 4934–4952). Blackwell Publishing Ltd. https://doi.org/10.1111/1462-2920.15274

O'Gorman, C. M., Fuller, H. T., & Dyer, P. S. (2009). Discovery of a sexual cycle in the opportunistic fungal pathogen Aspergillus fumigatus. *Nature*, *457*(7228), 471–474. https://doi.org/10.1038/nature07528

Paulussen, C., Hallsworth, J. E., Álvarez-Pérez, S., Nierman, W. C., Hamill, P. G., Blain, D., Rediers, H., & Lievens, B. (2017). Ecology of aspergillosis: insights into the pathogenic potency of Aspergillus fumigatus and some other Aspergillus species. In *Microbial Biotechnology* (Vol. 10, Issue 2). https://doi.org/10.1111/1751-7915.12367

Pearce, T. L., Wilson, C. R., Gent, D. H., & Scott, J. B. (2019). Multiple mutations across the succinate dehydrogenase gene complex are associated with boscalid resistance in Didymella tanaceti in pyrethrum. *PLoS ONE*, *14*(6). https://doi.org/10.1371/journal.pone.0218569

Peng, D., & Tarleton, R. (2015). Eupagdt: A web tool tailored to design crispr guide rnas for eukaryotic pathogens. *Microbial Genomics*, *1*(4). https://doi.org/10.1099/MGEN.0.000033

Pérez-Pérez, J. M., Candela, H., & Micol, J. L. (2009). Understanding synergy in genetic interactions. In *Trends in Genetics* (Vol. 25, Issue 8, pp. 368–376). https://doi.org/10.1016/j.tig.2009.06.004

Piotrowska, M. J., Fountaine, J. M., Ennos, R. A., Kaczmarek, M., & Burnett, F. J. (2017). Characterisation of Ramularia collo-cygni laboratory mutants resistant to succinate dehydrogenase inhibitors. *Pest Management Science*, *73*(6). https://doi.org/10.1002/ps.4442

Price, C. L., Parker, J. E., Warrilow, A. G., Kelly, D. E., & Kelly, S. L. (2015). Azole fungicides - understanding resistance mechanisms in agricultural fungal pathogens. *Pest Management Science*, *71*(8), 1054–1058. https://doi.org/10.1002/PS.4029

Rhodes, J. C. (2006). Aspergillus fumigatus: Growth and virulence. *Medical Mycology*, *44*(SUPPL. 1). https://doi.org/10.1080/13693780600779419

Ricroch, A., Harwood, W., Svobodová, Z., Sági, L., Hundleby, P., Badea, E. M., Rosca, I., Cruz, G., Salema Fevereiro, M. P., Marfà Riera, V., Jansson, S., Morandini, P., Bojinov, B.,

Cetiner, S., Custers, R., Schrader, U., Jacobsen, H. J., Martin-Laffon, J., Boisron, A., & Kuntz, M. (2016). Challenges facing European agriculture and possible biotechnological solutions. *Critical Reviews in Biotechnology*, *36*(5), 875–883. https://doi.org/10.3109/07388551.2015.1055707

Sallach, J. B., Thirkell, T. J., Field, K. J., & Carter, L. J. (2021). The emerging threat of human-use antifungals in sustainable and circular agriculture schemes. *Plants People Planet*, *3*(6), 685–693. https://doi.org/10.1002/ppp3.10222

Sang, H., & Lee, H. B. (2020). Molecular mechanisms of succinate dehydrogenase inhibitor resistance in phytopathogenic Fungi. In *Research in Plant Disease* (Vol. 26, Issue 1, pp. 1–7). The Korean Science & Technology Center. https://doi.org/10.5423/RPD.2020.26.1.1

Sen, P., Vijay, M., Singh, S., Hameed, S., & Vijayaraghavan, P. (2022). Understanding the environmental drivers of clinical azole resistance in Aspergillus species. In *Drug Target Insights* (Vol. 16, Issue 1, pp. 25–35). AboutScience Srl. https://doi.org/10.33393/dti.2022.2476

Shao, W., Sun, J., Zhang, X., & Chen, C. (2020). Amino acid polymorphism in succinate dehydrogenase subunit C involved in biological fitness of Botrytis cinerea. *Molecular Plant-Microbe Interactions*, *33*(4), 580–589. https://doi.org/10.1094/MPMI-07-19-0187-R

Shen, R., & Messer, P. W. (2022). Predicting the genomic resolution of bulk segregant analysis. *G3: Genes, Genomes, Genetics*, *12*(3). https://doi.org/10.1093/g3journal/jkac012

Shi, Y., Sun, B., Xie, X., Chai, A., Li, L., & Li, B. (2021). Site-directed mutagenesis of the succinate dehydrogenase subunits B and D from Corynespora cassiicola reveals different fitness costs and sensitivities to succinate dehydrogenase inhibitors. *Environmental Microbiology*, *23*(10). https://doi.org/10.1111/1462-2920.15361

Simões, K., Hawlik, A., Rehfus, A., Gava, F., & Stammler, G. (2018). First detection of a SDH variant with reduced SDHI sensitivity in Phakopsora pachyrhizi. *Journal of Plant Diseases and Protection*, *125*(1), 21–26. https://doi.org/10.1007/s41348-017-0117-5

Snelders, E., Huis In't Veld, R. A. G., Rijs, A. J. M. M., Kema, G. H. J., Melchers, W. J. G., & Verweij, P. E. (2009). Possible environmental origin of resistance of Aspergillus fumigatus to medical triazoles. *Applied and Environmental Microbiology*, *75*(12), 4053–4057. https://doi.org/10.1128/AEM.00231-09

Sugui, J. A., Kwon-Chung, K. J., Juvvadi, P. R., Latgé, J. P., & Steinbach, W. J. (2015). Aspergillus fumigatus and related species. *Cold Spring Harbor Perspectives in Medicine*, *5*(2). https://doi.org/10.1101/cshperspect.a019786

Sun, Y., Shi, H., Mao, C., Wu, J., & Zhang, C. (2021). Activity of a SDHI fungicide penflufen and the characterization of natural-resistance in Fusarium fujikuroi. *Pesticide Biochemistry and Physiology*, *179*. https://doi.org/10.1016/j.pestbp.2021.104960

van Rhijn, N., Furukawa, T., Zhao, C., McCann, B. L., Bignell, E., & Bromley, M. J. (2020). Development of a marker-free mutagenesis system using CRISPR-Cas9 in the pathogenic mould Aspergillus fumigatus. *Fungal Genetics and Biology*, *145*. https://doi.org/10.1016/j.fgb.2020.103479

Veloukas, T., Kalogeropoulou, P., Markoglou, A. N., & Karaoglanidis, G. S. (2014). Fitness and competitive ability of Botrytis cinerea field isolates with dual resistance to SDHI and QoI fungicides, associated with several sdhB and the cytb G143A mutations. *Phytopathology*, *104*(4). https://doi.org/10.1094/PHYTO-07-13-0208-R

Vielba-Fernández, A., Polonio, Á., Ruiz-Jiménez, L., de Vicente, A., Pérez-García, A., & Fernández-Ortuño, D. (2021). Resistance to the SDHI fungicides boscalid and fluopyram in podosphaera xanthii populations from commercial cucurbit fields in Spain. *Journal of Fungi*, *7*(9). https://doi.org/10.3390/jof7090733

Zhang, Y. (2008). I-TASSER server for protein 3D structure prediction. *BMC Bioinformatics*, *9*. https://doi.org/10.1186/1471-2105-9-40

Zulak, K. G., Farfan-Caceres, L., Knight, N. L., & Lopez-Ruiz, F. J. (2024). Exploiting long read sequencing to detect azole fungicide resistance mutations in Pyrenophora teres using unique molecular identifiers. *Scientific Reports*, *14*(1). https://doi.org/10.1038/s41598-024-56801-z